3.1 INTRODUCTION

Tris(hydroxymethyl)aminomethane (TRIS) is part of the aminoalcohol group and has found many applications in biochemistry, medicine, biology and physiology [Bubb *et al.*, 1995]. In biochemistry, TRIS is used as pH buffer in biological media as it has a pK_a value of 8.06. Therefore, TRIS buffer has an effective pH range between 7.0 and 9.2. It has also been reported that TRIS is used in the treatment of acidosis in acute lung injury and it is an effective method to control acidosis [Kallet *et al.*, 2000].

The main characteristic of TRIS is that it contains an amino group and three hydroxyl groups in the structure. The presence of the amino group allows the condensation with the carbonyl group; ketones or aldehydes which lead to the change in its physicochemical and biological properties. TRIS Schiff base derivatives are known to have a broad spectrum of biological activities including anti-tumour, antibiotic, anticancer, antihistamine, antifungal and anti-inflammatory effects. The biological activities of the complexes are found to be largely dependent on the tautomeric form of the ligand; and also the nature and position of the substituent in the benzene ring [Asgebom *et al.*, 1995, Chumakov *et al.*, 2003, Chumakov *et al.*, 2005, Odabaşoğlu *et al.*, 2003b].

The crystal structures of some of the *tris*(hydroxymethyl)aminomethane Schiff base ligands have been reported by several research groups [Odabaşoğlu *et al.*, 2003a, Chumakov *et al.*, 2000, Asgebom *et al.*, 1996, Tatar *et al.*, 2005]. The ligands are found to adopt the keto-amine tautomeric form whereby the hydrogen atom is located on the azomethine nitrogen atom. The N-H group and oxo-oxygen display a strong intramolecular N-H----O hydrogen in its structures. A recent X-ray study has shown that the Schiff base ligand, 4-chloro-2-[*tris*(hydroxymethyl)methyliminomethyl]phenol,

exists in zwitterionic form in solid state [Ng, 2008]. This report is in good agreement with the studies on salicylideneaniline structure which revealed that NH form of the salicylideneaniline is predominantly in a zwitterionic form in the crystal and is stabilized by electrostatic intermolecular interactions and further stabilized by intermolecular hydrogen bonding [Ogawa & Harada 2003].

In this study, a series of diorganotin complexes containing TRIS Schiff base ligands was prepared. The ligands and complexes were characterized by various spectroscopic techniques and further tested for their cytotoxic activities.

3.2 SYNTHESIS

The following commercial chemicals of reagent grade were used in the synthesis: *tris*(hydroxymethyl)aminomethane, salicylaldehyde, 5-bromosalicylaldehyde, 5-chlorosalicylaldehyde, 5-nitrosalicylaldehyde, 5-bromo-3-methoxy-2-hydroxy benzaldehyde, triethylamine, dimethyltin dichloride, dimethyltin oxide, dibutyltin dichloride, dibutyltin oxide, diphenyltin dichloride and diphenyltin oxide. The following organotin starting materials were prepared as discussed in chapter 2: dicyclohexyltin dichloride, dicyclohexyltin oxide, dibenzyltin dichloride, di(*o*-chlorobenzyl)tin dichloride and di(*p*-chlorobenzyl)tin dichloride.

The solvents used in the preparation of the Schiff base ligands and their complexes were absolute ethanol, chloroform and toluene. These solvents were distilled before use. Structural formula for the Schiff base ligands are listed in figure 3.1.

Figure 3.1.1
Structural formula for the TRIS Schiff base ligands

2-{[1,1-bis(hydroxymethyl)-2-oxidoethyl]iminomethyl}phenol, **TA**

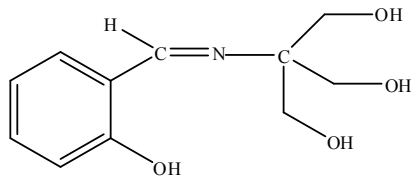

2-{[1,1-bis(hydroxymethyl)-2-oxidoethyl]iminomethyl}-4-bromophenol, **TB**

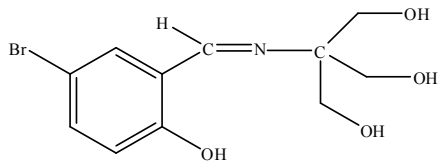

2-{[1,1-bis(hydroxymethyl)-2-oxidoethyl]iminomethyl}-4-chlorophenol, **TC**

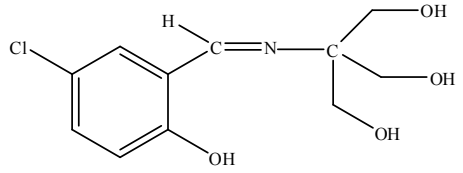

2-{[1,1-bis(hydroxymethyl)-2-oxidoethyl]iminomethyl}-4-nitrophenol, **TD**

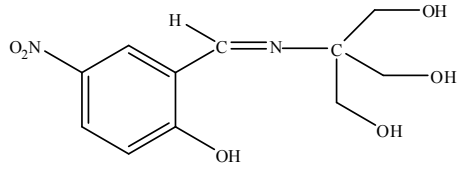

2-{[1,1-bis(hydroxymethyl)-2-oxidoethyl]iminomethyl}-2-methoxy-4-bromophenol, **TE**

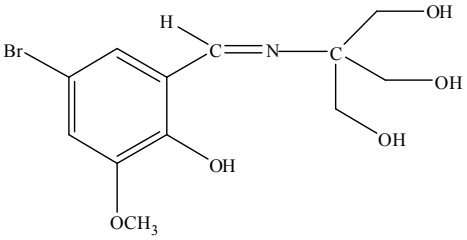

3.2.1 Preparation of Ligands

Preparation of 2-{[1,1-bis(hydroxymethyl)-2-oxidoethyl]iminomethyl}phenol, **TA**

Tris(hydroxymethyl)aminomethane (1.21 g, 0.01 mol) and salicylaldehyde (1.07 mL, 0.01 mol) were added to 100 mL of ethanol and the mixture was refluxed for 2 hours. A yellow solid formed upon cooling to room temperature. The solid was recrystallized from ethanol. Yield: 1.90 g (84.5 %) ; m.p. 139-140^{o}C

Preparation of 2-{[1,1-bis(hydroxymethyl)-2-oxidoethyl]iminomethyl}-4-bromophenol, **TB**

Tris(hydroxymethyl)aminomethane (1.21 g, 0.01 mol) and 5-bromosalicylaldehyde (2.01 g, 0.01 mol) were dissolved in 200 mL of ethanol. The mixture was refluxed for 2 hours. An orange solid formed when the solution was allowed to stand at room temperature. The solid was recrystallized from ethanol. Yield: 2.13 g (70.1 %) ; m.p. 141-142^{o}C

Preparation of 2-{[1,1-bis(hydroxymethyl)-2-oxidoethyl]iminomethyl}-4-chlorophenol, **TC**

A solution of *tris*(hydroxymethyl)aminomethane (1.21 g, 0.01 mol) was added to an ethanolic solution of 5-chlorosalicylaldehyde (1.57 g, 0.01 mol) and refluxed for 2 hours. The solution was allowed to stand at room temperature during which an orange solid formed and was recrystallized from ethanol. Yield: 1.95 g (75.1 %) ; m.p. 137-138^{o}C

Preparation of 2-{[1,1-bis(hydroxymethyl)-2-oxidoethyl]iminomethyl}-4-nitrophenol, **TD**

An ethanolic solution of 5-nitro-2-hydroxybenzaldehyde (1.67 g, 0.01 mol) was added to an ethanolic solution of *tris*(hydroxymethyl)aminomethane (1.21 g, 0.01 mol) and refluxed for 2 hours. A yellow solid formed when the solution was allowed to stand at room temperature. The solid was recrystallized from ethanol. Yield: 2.10 g (77.8 %) ; m.p. 228-230^{o}C

Preparation of 2-{[1,1-bis(hydroxymethyl)-2-oxidoethyl]iminomethyl}-2-methoxy-4-bromophenol, **TE**

A solution of *tris*(hydroxymethyl)aminomethane (1.21 g, 0.01 mol) was added to an ethanolic solution of 5-bromo-3-methoxy-2-hydroxybenzaldehyde (2.31 g, 0.01 mol) and refluxed for 2 hours. The solution was allowed to stand at room temperature during which an orange solid formed and was recrystallized from ethanol. Yield: 2.69 g (80.4%) ; m.p. 192-193^{o}C

3.2.2 Preparation of organotin complexes

Preparation of (2-{[1,1-bis(hydroxymethyl)-2-oxidoethyl]iminomethyl}phenolato)-dimethyltin(IV), **TA1**

To a suspension of dimethyltin oxide (0.17 g, 1.0 mmol) in dry toluene (40 ml), the ligand **TA** (0.22 g, 1.0 mmol) was added. The mixture was heated under reflux in a Dean-Stark apparatus for 8 hours for azeotropic removal of water formed in the reaction. The mixture was filtered and the filtrate was left at room temperature during which a yellow solid was obtained. Yield: 0.29 g (77.8 %) ; m.p. 196-198^{o}C

Preparation of (2-{[1,1-bis(hydroxymethyl)-2-oxidoethyl]iminomethyl}phenolato)-dibutyltin(IV), **TA2**

An ethanolic solution of dibutyltin dichloride (0.30 g, 1.0 mmol) was added to a hot ethanol solution containing ligand **TA** (0.22 g, 1.0 mmol) which was earlier refluxed with triethylamine (0.14 mL, 1.0 mmol). The solution was stirred and refluxed for 5 hours. The filtrate was evaporated until precipitation was obtained. The precipitation was recrystallised from toluene and the by-products, triethylammonium chloride, was removed through filtration. A yellow crystalline solid was obtained upon slow evaporation of the solution. Yield: 0.35 g (79.2 %) ; m.p. 126-127^{o}C

Preparation of (2-{[1,1-bis(hydroxymethyl)-2-oxidoethyl]iminomethyl}phenolato)-diphenyltin(IV), **TA3**

Ligand **TA** (0.22 g, 1.0 mmol) and triethylamine (0.14 mL, 1.0 mmol) were added to 100 mL of absolute ethanol and the mixture was heated under reflux for 2 hours. Diphenyltin dichloride (0.34 g, 1.0 mmol) was then added and the mixture was further refluxed for another 5 hours and filtered. The filtrate was evaporated until precipitation was obtained. The precipitation was recrystallised from toluene and the by-products, triethylammonium chloride, was removed through filtration. A yellow crystalline solid was obtained upon slow evaporation of the solution. Yield: 0.37 g (74.4%); m.p. >350^{o}C (dec.)

Preparation of (2-{[1,1-bis(hydroxymethyl)-2-oxidoethyl]iminomethyl}phenolato)-dicyclohexyltin(IV), **TA4**

A hot toluene solution of dicyclohexyltin oxide (0.30 g, 1.0 mmol) was added to a hot toluene solution containing ligand **TA** (0.22 g, 1.0 mmol). The mixture was stirred and refluxed using a Dean-Stark apparatus for 6 hours and the water formed was

removed at the end of the reaction. The mixture was filtered and the filtrate was left at room temperature during which a yellow solid was obtained. Yield: 0.37 g (75.5%) ; m.p. 190-191^{o}C

Preparation of (2-{[1,1-bis(hydroxymethyl)-2-oxidoethyl]iminomethyl}phenolato)-dibenzyltin(IV), **TA5**

Ligand **TA** (0.22 g, 1.0 mmol) and triethylamine (0.14 mL, 1.0 mmol) were dissolved in 100 mL of absolute ethanol and the mixture was heated under reflux for 2 hours. Dibenzyltin dichloride (0.37 g, 1.0 mmol) was then added and the mixture was refluxed for another 5 hours and filtered. The filtrate was evaporated until precipitation was obtained. The precipitation was recrystallised from toluene:chloroform (1:1) and the by-products, triethylammonium chloride, was removed through filtration. A yellow crystalline solid was obtained upon slow evaporation of the solution. Yield: 0.34 g (65.2%); m.p. >350^{o}C (dec.)

Preparation of (2-{[1,1-bis(hydroxymethyl)-2-oxidoethyl]iminomethyl}phenolato)-di(o-chlorobenzyltin)(IV), **TA6**

Ligand **TA** (0.22 g, 1.0 mmol) was refluxed with triethylamine (0.14 mL, 1.0 mmol) for 3 hours. Then, a hot ethanolic solution containing di(*o*-chlorobenzyl)tin dichloride (0.44 g, 2.0 mmol) was added to the mixture. The mixture was stirred, refluxed for 5 hours and filtered. The filtrate was evaporated until precipitation was obtained. The precipitation was recrystallised from toluene and the by-products, triethylammonium chloride, was removed through filtration. A yellow crystalline solid was obtained upon slow evaporation of the solution. Yield: 0.42 g (70.3%); m.p. 194-195^{o}C

Preparation of (2-{[1,1-bis(hydroxymethyl)-2-oxidoethyl]iminomethyl}phenolato)-di(p-chlorobenzyltin)(IV), **TA7**

An ethanolic solution containing ligand **TA** (0.22 g, 1.0 mmol) was refluxed with triethylamine (0.14 mL, 1.0 mmol) for 2 hours. Then, a hot ethanolic solution containing di(*p*-chlorobenzyl)tin dichloride (0.44 g, 1.0 mmol) was added to the mixture, refluxed for 6 hours and filtered. The filtrate was evaporated until precipitation was obtained. The precipitation was recrystallised from toluene and the by-products, triethylammonium chloride, was removed through filtration. A yellow crystalline solid was obtained upon slow evaporation of the solution.Yield: 0.39 g (65.0 %) ; m.p. > 350^{o}C (dec.)

The various complexes were prepared using the similar procedure described for complexes **TA1**-**TA7**. The yields and melting points of the complexes are tabulated in table 3.3.2.

3.2.3 Physical measurement of the Schiff base ligands and organotin complexes

The melting points of the compounds were determined on a 'Electrothermal' digital melting point apparatus and were uncorrected. Elemental analyses of the complexes were carried out on an Eager 300 CHNS Elemental Analyzer in the Department of Chemistry, National University of Malaysia and on a Perkin-Elmer EA2400 CHNS Elemental Analyzer in the University of Malaya.

The infrared spectra for the compounds were recorded in the region 400-4000 cm^{-1} with a Perkin-Elmer Spectrum 2000 FT-IR spectrophotometer and a Perkin-Elmer Spectrum RX1 FT-IR spectrophotometer. The samples were prepared as nujol mull or KBr pellet. The UV spectra for the ligands and organotin complexes were recorded

using a Shimadzu UV-PC1601 UV-visible spectrophotometer in the wavelength range of 190 to 600 nm.

The ^{1}H and ^{13}C NMR spectra for the ligands were recorded in $CDCl_3$ or deuterated DMSO at ambient temperature on a JEOL JNM-GSX270 FT NMR SYSTEM spectrometer operating at 270.05 MHz for ^{1}H NMR and 67.80 MHz for ^{13}C NMR. The ^{119}Sn NMR spectra were recorded on a JEOL ECA-400MHz. The chemical shifts were recorded in ppm with reference to Me_4Si for ^{1}H NMR, $CDCl_3$ and DMSO for ^{13}C NMR and Me_4Sn for ^{119}Sn NMR. The ^{1}H and ^{13}C NMR spectra of some of the complexes in DMSO gave poor spectra and hence, assignment of peaks was not satisfactory.

The X-ray crystallographic intensity data were measured using Mo-K_α radiation graphite-crystal monochromator (λ= 0.71073Å) radiation on a Bruker SMART APEX2 CCD diffractometer in University of Malaya and Bruker-Nonius APEX2 CCD diffractometer in University of Canterbury, New Zealand. The structure of the compounds were solved by the direct method and refined by the full-matrix least-squares procedure based on F^2 using the SHELXL programme. Supplementary data including observed and calculated structure factors for the complexes are available from the author on request.

3.3 RESULTS AND DISCUSSION

3.3.1 Analytical Data

The TRIS Schiff base ligands were prepared from the reactions of 1:1 molar ratio of the *tris*(hydroxymethyl)aminomethane with salicylaldehyde and substituted salicylaldehyde. However, pure products were not isolated from the reaction between the *tris*(hydroxymethyl)aminomethane with 2-hydroxyacetophenone and substituted 2-hydroxyacetophenone. As the obtained product was a sticky mass, purification failed to give moderate yield of the product.

The prepared TRIS Schiff base had several potential coordination sites namely the imine nitrogen and four hydroxyl groups; three hydroxyl groups on the methylene group and one hydroxyl on the salicylaldehyde or substituted salicylaldehyde site. A general reaction scheme of the preparation of the Schiff base ligands is shown in scheme 3.3.1.

Scheme 3.3.1 Reaction scheme for the preparation of the TRIS Schiff base ligands

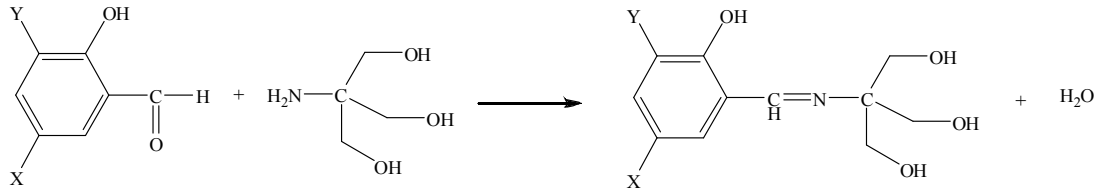

X = -H, -Br, -Cl; Y = -H, -OCH_3

The Schiff base ligands were used without further purification in the preparation of their organotin complexes. The analytical data of the Schiff base ligands, **TA**, **TB**, **TC**, **TD** and **TE** are listed in table 3.3.1. The colour of the Schiff base ligands were yellow or orange and their melting points were in the range of 137-230^{o}C. As

diorganotin halides and diorganotin oxides are relatively strong Lewis acids, they can easily form stable complexes with Schiff bases. The diorganotin complexes obtained were yellow, orange or brown in colour. A general reaction scheme for the preparation of the complexes is shown in scheme 3.3.2.

Scheme 3.3.2 Reaction scheme for the preparation of the diorganotin TRIS Schiff base complexes

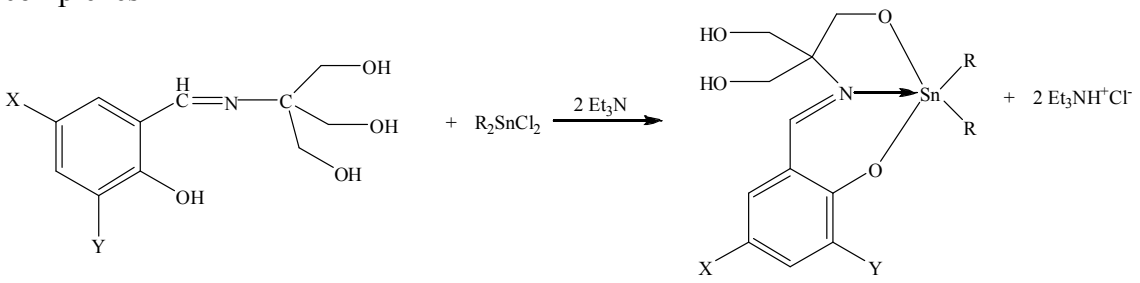

X = H, Br, Cl; Y = OCH_3
R = CH_3, n-C_4H_9, C_6H_5, benzyl, *o*-Clbenzyl, *p*-Clbenzyl

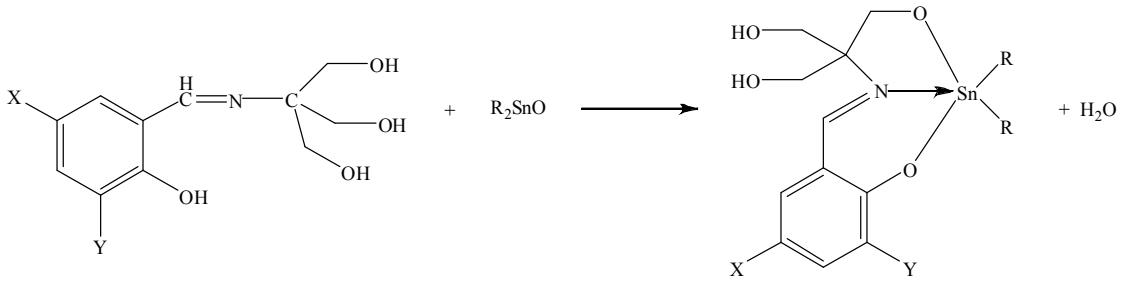

X = H, Br, Cl; Y = OCH_3
R = CH_3, *n*-C_4H_9, C_6H_5, Cy

Table 3.3.1.
Analytical data for the TRIS ligands

Ligand	Colour	Percentage Yield (%)	Melting-Point (^{o}C)	Elemental Analysis Found (Calculated) (%)		
				C	H	N
2-{[1,1-*Bis*(hydroxymethyl)-2-oxidoethyl]-iminomethyl}phenol, **TA**	Yellow	84.5	139-140	58.11 (58.69)	6.33 (6.66)	5.70 (6.21)
2-{[1,1-*Bis*(hydroxymethyl)-2-oxidoethyl]-iminomethyl}-4-bromophenol, **TB**	Orange	70.1	141-142	43.01 (43.48)	4.60 (4.61)	4.49 (4.61)
2-{[1,1-*Bis*(hydroxymethyl)-2-oxidoethyl]-iminomethyl}-4-chlorophenol, **TC**	Orange	75.1	137-138	51.18 (50.89)	5.42 (5.39)	4.91 (5.39)
2-{[1,1-*Bis*(hydroxymethyl)-2-oxidoethyl]-iminomethyl}-4-nitrophenol, **TD**	Yellow	77.8	228-230	48.71 (48.89)	5.20 (5.18)	9.97 (10.36)
2-{[1,1-*Bis*(hydroxymethyl)-2-oxidoethyl]-iminomethyl}-2-methoxy-4-bromophenol, **TE**	Yellow	80.4	192-193	43.01 (43.13)	4.74 (4.79)	3.90 (4.19)

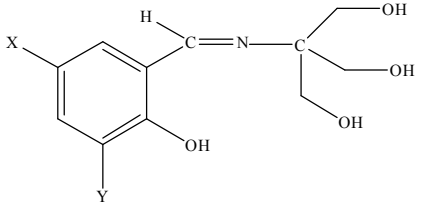

TA: X = H, Y= H ; **TB**: X = Br, Y = H;
TC: X = Cl, Y = H; **TD**: X = NO_2, Y = H;
TE: X= Br, Y = OCH_3

Table 3.3.2a
Analytical data for (2-{[1,1-*bis*(hydroxymethyl)-2-oxidoethyl]iminomethyl}phenolato)diorganotin complexes

Complex	Colour	Percentage Yield (%)	Melting-Point (^{o}C)	Elemental Analysis Found (Calculated) (%)		
				C	H	N
(2-{[1,1-Bis(hydroxymethyl)-2-oxidoethyl]-iminomethyl}phenolato)dimethyltin(IV), **TA1**	Yellow	77.8	196-198	41.02 (41.99)	5.02 (5.11)	3.98 (3.77)
(2-{[1,1-Bis(hydroxymethyl)-2-oxidoethyl]-iminomethyl}phenolato)dibutyltin(IV), **TA2**	Yellow	79.2	126-127	49.94 (50.06)	7.12 (6.80)	2.79 (3.07)
(2-{[1,1-Bis(hydroxymethyl)-2-oxidoethyl]-iminomethyl}phenolato)diphenyltin(IV), **TA3**	Yellow	74.4	>350 (dec.)	56.00 (55.69)	4.66 (4.64)	2.73 (2.82)
(2-{[1,1-Bis(hydroxymethyl)-2-oxidoethyl]-iminomethyl}phenolato)dicyclohexyltin(IV), **TA4**	Yellow	75.5	190-191	53.70 (54.39)	6.87 (6.89)	3.02 (2.76)
(2-{[1,1-Bis(hydroxymethyl)-2-oxidoethyl]-iminomethyl}phenolato)dibenzyltin(IV), **TA5**	Yellow	65.2	> 350 (dec.)	56.95 (57.31)	5.57 (5.15)	2.43 (2.67)
(2-{[1,1-Bis(hydroxymethyl)-2-oxidoethyl]-iminomethyl}phenolato)-di(*o*-chlorobenzyl)tin(IV), **TA6**	Yellow	70.3	194-195	51.15 (50.64)	4.27 (4.22)	2.38 (2.36)
(2-{[1,1-Bis(hydroxymethyl)-2-oxidoethyl]-iminomethyl}phenolato)-di(*p*-chlorobenzyl)tin(IV), **TA7**	Yellow	65.0	> 350 (dec.)	50.35 (50.64)	3.90 (4.22)	2.20 (2.36)

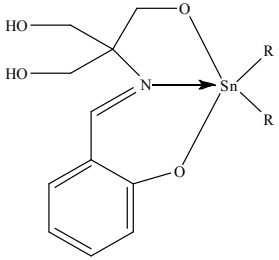

R = CH_3, C_4H_9, phenyl (Ph), cyclohexyl (Cy), benzyl (Bz), *o*-chlorobenzyl (*o*-ClBz), *p*-chlorobenzyl (*p*-ClBz)

Table 3.3.2b
Analytical data for (2-{[1,1-*bis*(hydroxymethyl)-2-oxidoethyl]iminomethyl}-4-bromophenolato)diorganotin complexes

Complex	Colour	Percentage Yield (%)	Melting-Point (^{o}C)	Elemental Analysis Found (Calculated) (%)		
				C	H	N
Bis[(2-{[1,1-*Bis*(hydroxymethyl)-2-oxidoethyl]-iminomethyl}-4-bromophenolato)]-dimethyltin(IV), **TB1**	Yellow	72.1	208-210	34.29 (34.65)	3.89 (3.99)	3.34 (3.11)
(2-{[1,1-*Bis*(hydroxymethyl)-2-oxidoethyl]-iminomethyl}-4-bromophenolato)dibutyltin(IV), **TB2**	Yellow	78.5	110-112	42.84 (42.78)	5.69 (5.62)	2.42 (2.62)
(2-{[1,1-*Bis*(hydroxymethyl)-2-oxidoethyl]-iminomethyl}-4-bromophenolato)-diphenyltin(IV), **TB3**	Yellow	70.5	> 350 (dec.)	48.07 (48.16)	3.79 (3.84)	2.86 (2.44)
(2-{[1,1-*Bis*(hydroxymethyl)-2-oxidoethyl]--iminomethyl}-4-bromophenolato)-dicyclohexyltin(IV), **TB4**	Yellow	71.1	194-196	47.32 (47.07)	5.27 (5.79)	2.78 (2.31)
(2-{[1,1-Bis(hydroxymethyl)-2-oxidoethyl]-iminomethyl}-4-bromophenolato)-dibenzyltin(IV), **TB5**	Yellow	73.2	> 350 (dec.)	50.29 (49.81)	4.40 (4.31)	2.55 (2.32)
(2-{[1,1-Bis(hydroxymethyl)-2-oxidoethyl]-iminomethyl}-4-bromophenolato)-di(*o*-chlorobenzyl)tin(IV), **TB6**	Yellow	70.1	> 350 (dec.)	45.00 (44.69)	3.61 (3.59)	1.91 (2.08)
(2-{[1,1-Bis(hydroxymethyl)-2-oxidoethyl]-iminomethyl}-4-bromophenolato)-di(*p*-chlorobenzyl)tin(IV), **TB7**	Yellow	70.3	212-214	45.02 (44.69)	3.90 (3.59)	2.35 (2.08)

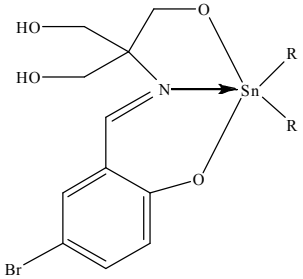

R = CH_3, C_4H_9, phenyl (Ph), cyclohexyl (Cy), benzyl (Bz), *o*-chlorobenzyl (*o*-ClBz), *p*-chlorobenzyl (*p*-ClBz)

Table 3.3.2c
Analytical data for (2-{[1,1-*bis*(hydroxymethyl)-2-oxidoethyl]iminomethyl}-4-chlorophenolato)diorganotin complexes

Complex	Colour	Percentage Yield (%)	Melting-Point (^{o}C)	Elemental Analysis Found (Calculated) (%)		
				C	H	N
(2-{[1,1-*Bis*(hydroxymethyl)-2-oxidoethyl]-iminomethyl}-4-chlorophenolato)-dimethyltin(IV), **TC1**	Yellow	79.9	220-222	38.79 (38.72)	4.00 (4.43)	3.80 (3.44)
(2-{[1,1-*Bis*(hydroxymethyl)-2-oxidoethyl]-iminomethyl}-4-chlorophenolato)dibutyltin(IV), **TC2**	Yellow	82.5	133-134	46.34 (46.52)	5.99 (6.11)	3.02 (2.85)
(2-{[1,1-*Bis*(hydroxymethyl)-2-oxidoethyl]-iminomethyl}-4-chlorophenolato)-diphenyltin(IV), **TC3**	Yellow	72.3	> 350 (dec.)	52.27 (52.10)	3.99 (4.15)	2.65 (2.64)
(2-{[1,1-*Bis*(hydroxymethyl)-2-oxidoethyl]-iminomethyl}-4-chlorophenolato)-dicyclohexyltin(IV), **TC4**	Yellow	78.9	180-182	50.59 (50.93)	5.89 (6.27)	2.70 (2.58)
(2-{[1,1-*Bis*(hydroxymethyl)-2-oxidoethyl]-iminomethyl}-4-chlorophenolato)dibenzyltin(IV), **TC5**	Yellow	73.2	> 350 (dec.)	53.38 (53.81)	4.30 (4.66)	2.67 (2.51)
(2-{[1,1-*Bis*(hydroxymethyl)-2-oxidoethyl]-iminomethyl}-4-chlorophenolato)-di(*o*-chlorobenzyl)tin(IV), **TC6**	Yellow	72.1	188-189	48.15 (47.89)	3.97 (3.83)	2.45 (2.23)
(2-{[1,1-*Bis*(hydroxymethyl)-2-oxidoethyl]-iminomethyl}-4-chlorophenolato)-di(*p*-chlorobenzyl)tin(IV), **TC7**	Yellow	66.2	>350 (dec.)	47.50 (47.89)	3.47 (3.83)	2.03 (2.23)

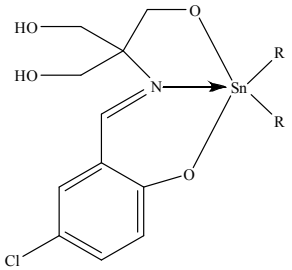

R = CH_3, C_4H_9, phenyl (Ph), cyclohexyl (Cy), benzyl (Bz), *o*-chlorobenzyl (*o*-ClBz), *p*-chlorobenzyl (*p*-ClBz)

Table 3.3.2d
Analytical data for (2-{[1,1-*bis*(hydroxymethyl)-2-oxidoethyl]iminomethyl}-4-nitrophenolato)diorganotin complexes

Complex	Colour	Percentage Yield (%)	Melting-Point (^{o}C)	Elemental Analysis Found (Calculated) (%)		
				C	H	N
(2-{[1,1-*Bis*(hydroxymethyl)-2-oxidoethyl]-iminomethyl}-4-nitrophenolato)dimethyltin(IV), **TD1**	Yellow	78.1	113-114	36.99 (37.45)	4.59 (4.32)	6.68 (6.72)
(2-{[1,1-*Bis*(hydroxymethyl)-2-oxidoethyl]-iminomethyl}-4-nitrophenolato)dibutyltin(IV), **TD2**	Yellow	73.5	97-98	45.10 (45.55)	5.92 (5.99)	5.77 (5.59)
(2-{[1,1-*Bis*(hydroxymethyl)-2-oxidoethyl]-iminomethyl}-4-nitrophenolato)diphenyltin(IV), **TD3**	Yellow	73.8	179-180	50.77 (51.05)	4.28 (4.07)	5.07 (5.17)
(2-{[1,1-*Bis*(hydroxymethyl)-2-oxidoethyl]-iminomethyl}-4-nitrophenolato)-dicyclohexyltin(IV), **TD4**	Yellow	77.6	210-212	50.28 (49.95)	6.08 (6.33)	5.34 (5.06)
(2-{[1,1-*Bis*(hydroxymethyl)-2-oxidoethyl]-iminomethyl}-4-nitrophenolato)dibenzyltin(IV), **TD5**	Orange	70.1	90-91	53.05 (52.76)	4.82 (4.57)	5.26 (4.92)
(2-{[1,1-*Bis*(hydroxymethyl)-2-oxidoethyl]-iminomethyl}-4-nitrophenolato)-di(*o*-chlorobenzyl)tin(IV), **TD6**	Orange	71.2	102-103	47.84 (47.06)	3.59 (3.76)	4.00 (4.39)
(2-{[1,1-*Bis*(hydroxymethyl)-2-oxidoethyl]-iminomethyl}-4-nitrophenolato)-di(*p*-chlorobenzyl)tin(IV), **TD7**	Orange	69.3	72-74	47.77 (47.06)	3.76 (3.76)	4.28 (4.39)

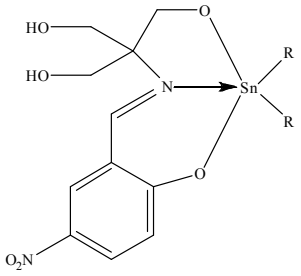

R = CH_3, C_4H_9, phenyl (Ph), cyclohexyl (Cy), benzyl (Bz), *o*-chlorobenzyl (*o*-ClBz), *p* -chlorobenzyl (*p*-ClBz)

Table 3.3.2e
Analytical data for (2-{[1,1-*bis*(hydroxymethyl)-2-oxidoethyl]iminomethyl}-2-methoxy-4-bromophenolato)diorganotin complexes

Complex	Colour	Percentage Yield (%)	Melting-Point (^{o}C)	Elemental Analysis Found (Calculated) (%)		
				C	H	N
(2-{[1,1-*Bis*(hydroxymethyl)-2-oxidoethyl]-iminomethyl}-2-methoxy-4-bromophenolato)-dimethyltin(IV), **TE2**	Yellow	78.8	179-180	35.22 (34.97)	4.10 (4.16)	2.93 (2.91)
(2-{[1,1-*Bis*(hydroxymethyl)-2-oxidoethyl]-iminomethyl}-2-methoxy-4-bromophenolato)-dibutyltin(IV), **TE2**	Yellow	72.2	145-146	42.48 (42.50)	5.41 (5.66)	2.46 (2.48)
(2-{[1,1-*Bis*(hydroxymethyl)-2-oxidoethyl]-iminomethyl}-2-methoxy-4-bromophenolato)-diphenyltin(IV), **TE3**	Yellow	71.5	208-210	47.90 (47.64)	4.24 (3.97)	2.32 (2.31)
(2-{[1,1-*Bis*(hydroxymethyl)-2-oxidoethyl]-iminomethyl}-2-methoxy-4-bromophenolato)-dicyclohexyltin(IV), **TE4**	Yellow	76.8	180-181	46.80 (46.72)	5.54 (5.83)	2.42 (2.27)
(2-{[1,1-*Bis*(hydroxymethyl)-2-oxidoethyl]-iminomethyl}-2-methoxy-4-bromophenolato)-dibenzyltin(IV), **TE5**	Yellow	72.2	162-164	48.99 (49.33)	4.75 (4.42)	2.56 (2.21)
(2-{[1,1-*Bis*(hydroxymethyl)-2-oxidoethyl]-iminomethyl}-2-methoxy-4-bromophenolato)-di(*o*-chlorobenzyl)tin(IV), **TE6**	Yellow	70.3	167-168	44.68 (44.48)	3.80 (3.70)	1.95 (1.99)
(2-{[1,1-*Bis*(hydroxymethyl)-2-oxidoethyl]-iminomethyl}-2-methoxy-4-bromophenolato)-di(*p*-chlorobenzyl)tin(IV), **TE7**	Yellow	69.6	92-95	44.81 (44.48)	3.42 (3.70)	1.64 (1.99)

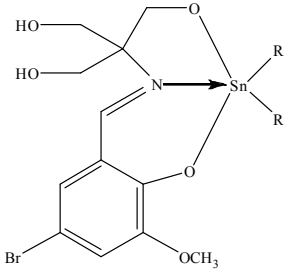

R = CH_3, C_4H_9, phenyl (Ph), cyclohexyl (Cy), benzyl (Bz), *o*-chlorobenzyl (*o*-ClBz), *p*-chlorobenzyl (*p*-ClBz)

3.3.2 IR Spectral data

Table 3.3.3 summarizes the characteristic infrared stretching frequencies for ligands **TA**, **TB**, **TC**, **TD** and **TE** while the vibrational stretching frequencies for the diorganotin complexes are listed in table 3.3.4. The hydroxyl stretching frequencies of the free ligands were expected to be in the 3200-3400 cm^{-1} region [Mikhalylova *et al.*, 2006, Sandbhlor *et al.*, 2002] and a strong broad peak was observed around 3290 cm^{-1} in the ligands spectra. However, no visible N-H stretching was observed, possibly due to the overlapping of the N-H stretching frequency with the O-H stretching frequency. In the diorganotin complexes, a characteristic absorption was also clearly observed between 3200-3400 cm^{-1} region which indicated that not all the hydroxyl oxygen atoms participated in the coordination to the centre metal atom [Dey *et al.*, 1982, Yin and Chen 2006a, Sui *et al.*, 2007]. These findings supported the molecular structure of the diorganotin complexes obtained from X-ray crystallography.

All the Schiff base ligands exhibited the C=N stretching frequencies in the region of 1635-1650 cm^{-1} as derived from the azomethine group and this was within the range reported for azomethine group in Schiff base ligands [Sandbhor *et al.*, 2002, Sui *et al.*, 2007]. The C=N stretching frequencies for the organotin complexes were found in the region between 1608-1620 cm^{-1} which was about 20-30 cm^{-1} lower than those reported for the Schiff base ligands. These findings confirmed the involvement of the azomethine nitrogen in the coordination with tin atom. The weakening in the C=N bond led to the lowering of the C=N stretching frequencies in the diorganotin complexes. The reason for this was due to the reduction in the electron density of the azomethine nitrogen and carbonyl moieties.

The C-O stretching frequencies for both the ligands and diorganotin complexes were within the region 1150-1200 cm^{-1} [Signorini *et al.*, 1996, Faniran *et al.*, 1974, Bellamy, 1958]. Ligand **TE** and its diorganotin complexes exhibited an asymmetrical and symmetrical *v*(C-O-C) vibration stretching in the 1147-1223 cm^{-1} and 1026-1097 cm^{-1} region.

The presence of two new bands was observed in the lower frequency region of 400-800 cm^{-1} for the organotin complexes. The medium absorption in the region of 680-710 cm^{-1} had been assigned to the Sn-O stretching mode of vibration while the weak absorption in the region of 460-480 cm^{-1} had been assigned to the Sn-N stretching vibration. Both the Sn-O and Sn-N stretching frequencies were within the range reported for diorganotin derivatives [Pettinari *et al.*, 2001, Shujha *et al.*, 2010]

Table 3.3.3
Infrared spectral data for the TRIS ligands

Ligand	*v*(O-H, N-H)	*v*(C=N)	*v*(-O-C=C-)	*v*(C-O)	v_a(C-O-C), v_s(C-O-C)
2-{[1,1-*Bis*(hydroxymethyl)-2-oxidoethyl]-iminomethyl}phenol, **TA**	3321b	1636s	1555m	1189m	-
2-{[1,1-*Bis*(hydroxymethyl)-2-oxidoethyl]-iminomethyl}-4-bromophenol, **TB**	3357b	1637s	1560m	1175m	-
2-{[1,1-*Bis*(hydroxymethyl)-2-oxidoethyl]-iminomethyl}-4-chlorophenol, **TC**	3339b	1639s	1561m	1175m	-
2-{[1,1-*Bis*(hydroxymethyl)-2-oxidoethyl]-iminomethyl}-4-nitrophenol, **TD**	3255b	1650s	1545m	1194m	-
2-{[1,1-*Bis*(hydroxymethyl)-2-oxidoethyl]-iminomethyl}-2-methoxy-4-bromophenol, **TE**	3330b	1640s	1528m	1171m	1066m

[a] s = strong, m = medium, w = weak, sh = shoulder, b = broad

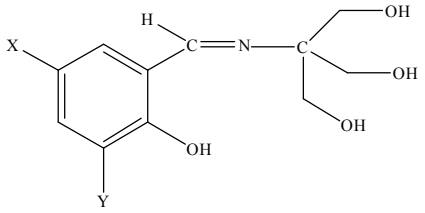

TA: X = H, Y= H ; **TB**: X = Br, Y = H;
TC: X = Cl, Y = H; **TD**: X = NO_2, Y = H;
TE: X= Br, Y = OCH_3

Table 3.3.4a
Infrared spectral data for (2-{[1,1-*bis*(hydroxymethyl)-2-oxidoethyl]iminomethyl}phenolato)diorganotin complexes

Complex	*v*(O-H)	*v*(C=N)	*v*(-O-C=C-)	*v*(C-O)	*v*(Sn-O)	*v*(Sn-N)
(2-{[1,1-*Bis*(hydroxymethyl)-2-oxidoethyl]-iminomethyl}phenolato)dimethyltin(IV), **TA1**	3495b	1614	1540m	1191m	669m	419w
(2-{[1,1-*Bis*(hydroxymethyl)-2-oxidoethyl]-iminomethyl}phenolato)dibutyltin(IV), **TA2**	3422b	1611s	1541m	1182m	678w	422w
(2-{[1,1-*Bis*(hydroxymethyl)-2-oxidoethyl]-iminomethyl}phenolato)diphenyltin(IV), **TA3**	3281b	1611s	1545m	1173m	699w	436w
(2-{[1,1-*Bis*(hydroxymethyl)-2-oxidoethyl]-iminomethyl}phenolato)dicyclohexyltin(IV), **TA4**	3369b	1616s	1542m	1149m	669w	421w
(2-{[1,1-*Bis*(hydroxymethyl)-2-oxidoethyl]-iminomethyl}phenolato)dibenzyltin(IV), **TA5**	3401b	1612s	1545m	1174m	698m	458w
(2-{[1,1-*Bis*(hydroxymethyl)-2-oxidoethyl]-iminomethyl}phenolato)di(*o*-chlorobenzyl)tin(IV), **TA6**	3373b	1609s	1539m	1140m	697w	457w
(2-{[1,1-*Bis*(hydroxymethyl)-2-oxidoethyl]-iminomethyl}phenolato)di(*p*-chlorobenzyl)tin(IV), **TA7**	3282b	1610s	1543m	1172m	688w	412w

[a] s = strong, m = medium, w = weak, sh = shoulder, b = broad

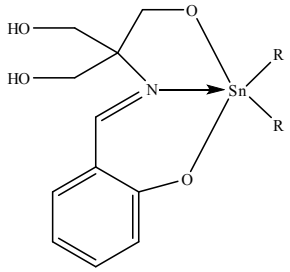

R = CH_3, C_4H_9, phenyl (Ph), cyclohexyl (Cy), benzyl (Bz), *o*-chlorobenzyl (*o*-ClBz), *p* -chlorobenzyl (*p*-ClBz)

Table 3.3.4b
Infrared spectral data for (2-{[1,1-*bis*(hydroxymethyl)-2-oxidoethyl]iminomethyl}-4-bromophenolato)diorganotin complexes

Complex	*v*(O-H)	*v*(C=N)	*v*(-O-C=C-)	*v*(C-O)	*v*(Sn-O)	*v*(Sn-N)
Bis[(2-{[1,1-*Bis*(hydroxymethyl)-2-oxidoethyl]-iminomethyl}-4-bromophenolato)]dimethyltin(IV), **TB1**	3293b	1612s	1525m	1169m	684m	455w
(2-{[1,1-*Bis*(hydroxymethyl)-2-oxidoethyl]-iminomethyl}-4-bromophenolato)dibutyltin(IV), **TB2**	3290b	1612s	1528m	1169m	661m	451w
(2-{[1,1-*Bis*(hydroxymethyl)-2-oxidoethyl]-iminomethyl}-4-bromophenolato)diphenyltin(IV), **TB3**	3380b	1608s	1528m	1177m	660m	448w
(2-{[1,1-*Bis*(hydroxymethyl)-2-oxidoethyl]-iminomethyl}-4-bromophenolato)dicyclohexyltin(IV), **TB4**	3369b	1612s	1525m	1172m	658m	434w
(2-{[1,1-*Bis*(hydroxymethyl)-2-oxidoethyl]-iminomethyl}-4-bromophenolato)dibenzyltin(IV), **TB5**	3373b	1618s	1531m	1172m	657m	463w
(2-{[1,1-*Bis*(hydroxymethyl)-2-oxidoethyl]-iminomethyl}-4-bromophenolato)-di(*o*-chlorobenzyl)tin(IV), **TB6**	3339b	1620s	1552m	1177m	655m	455w
(2-{[1,1-*Bis*(hydroxymethyl)-2-oxidoethyl]-iminomethyl}-4-bromophenolato)-di(*p*-chlorobenzyl)tin(IV), **TB7**	3285b	1611s	1531m	1167m	653m	420w

[a] s = strong, m = medium, w = weak, sh = shoulder, b = broad

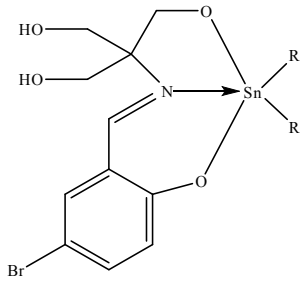

R = CH_3, C_4H_9, phenyl (Ph), cyclohexyl (Cy), benzyl (Bz), *o*-chlorobenzyl (*o*-ClBz), *p*-chlorobenzyl (*p*-ClBz)

Table 3.3.4c
Infrared spectral data for (2-{[1,1-*bis*(hydroxymethyl)-2-oxidoethyl]iminomethyl}-4-chlorophenolato)diorganotin complexes

Complex	*v*(O-H)	*v*(C=N)	*v*(-O-C=C-)	*v*(C-O)	*v*(Sn-O)	*v*(Sn-N)
(2-{[1,1-*Bis*(hydroxymethyl)-2-oxidoethyl]-iminomethyl}-4-chlorophenolato)dimethyltin(IV), **TC1**	3376b	1618s	1529m	1180m	702w	430w
(2-{[1,1-*Bis*(hydroxymethyl)-2-oxidoethyl]-iminomethyl}-4-chlorophenolato)dibutyltin(IV), **TC2**	3327b	1614s	1533m	1170m	690m	414w
(2-{[1,1-*Bis*(hydroxymethyl)-2-oxidoethyl]-iminomethyl}-4-chlorophenolato)diphenyltin(IV), **TC3**	3380b	1611s	1532m	1178m	698m	431m
(2-{[1,1-*Bis*(hydroxymethyl)-2-oxidoethyl]-iminomethyl}-4-chlorophenolato)dicyclohexyltin(IV), **TC4**	3367b	1617s	1528m	1172m	702m	435w
(2-{[1,1-*Bis*(hydroxymethyl)-2-oxidoethyl]-iminomethyl}-4-chlorophenolato)dibenzyltin(IV), **TC5**	3399b	1619s	1535m	1170m	700m	467w
(2-{[1,1-*Bis*(hydroxymethyl)-2-oxidoethyl]-iminomethyl}-4-chlorophenolato)-di(*o*-chlorobenzyl)tin(IV), **TC6**	3370b	1620s	1533m	1180m	699m	437w
(2-{[1,1-*Bis*(hydroxymethyl)-2-oxidoethyl]-iminomethyl}-4-chlorophenolato)-di(*p*-chlorobenzyl)tin(IV), **TC7**	3283b	1614s	1535m	1167m	700m	430w

[a] s = strong, m = medium, w = weak, sh = shoulder, b = broad

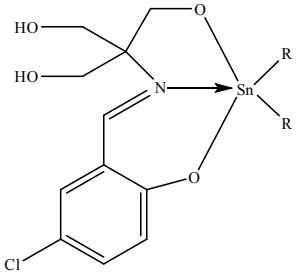

R = CH_3, C_4H_9, phenyl (Ph), cyclohexyl (Cy), benzyl (Bz), *o*-chlorobenzyl (*o*-ClBz), *p*-chlorobenzyl (*p*-ClBz)

Table 3.3.4d
Infrared spectral data for (2-{[1,1-*bis*(hydroxymethyl)-2-oxidoethyl]iminomethyl}-4-nitrophenolato)diorganotin complexes

Complex	*v*(O-H)	*v*(C=N)	*v*(-O-C=C-)	*v*(C-O)	*v*(Sn-O)	*v*(Sn-N)
(2-{[1,1-*Bis*(hydroxymethyl)-2-oxidoethyl]-iminomethyl}-4-nitrophenolato)dimethyltin(IV), **TD1**	3294b	1619s	1546m	1172m	695w	448w
(2-{[1,1-*Bis*(hydroxymethyl)-2-oxidoethyl]-iminomethyl}-4-nitrophenolato)dibutyltin(IV), **TD2**	3274b	1617m	1543m	1172m	728w	450w
(2-{[1,1-*Bis*(hydroxymethyl)-2-oxidoethyl]-iminomethyl}-4-nitrophenolato)diphenyltin(IV), **TD3**	3396b	1615s	1554m	1187m	692m	448w
(2-{[1,1-*Bis*(hydroxymethyl)-2-oxidoethyl]-iminomethyl}-4-nitrophenolato)dicyclohexyltin(IV), **TD4**	3274b	1617s	1545m	1173m	729w	485w
(2-{[1,1-*Bis*(hydroxymethyl)-2-oxidoethyl]-iminomethyl}-4-nitrophenolato)dibenzyltin(IV), **TD5**	3262b	1615s	1545m	1155m	729w	458w
(2-{[1,1-*Bis*(hydroxymethyl)-2-oxidoethyl]-iminomethyl}-4-nitrophenolato)-di(*o*-chlorobenzyl)tin(IV), **TD6**	3254b	1617s	1548m	1156m	730w	455w
(2-{[1,1-*Bis*(hydroxymethyl)-2-oxidoethyl]-iminomethyl}-4-nitrophenolato)-di(*p*-chlorobenzyl)tin(IV), **TD7**	3422b	1616m	1546m	1173m	730m	460w

[a] s = strong, m = medium, w = weak, sh = shoulder, b = broad

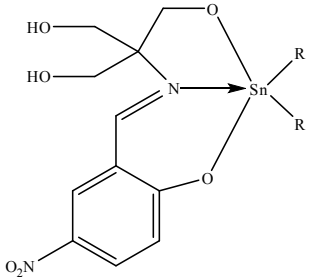

R = CH_3, C_4H_9, phenyl (Ph), cyclohexyl (Cy), benzyl (Bz), *o*-chlorobenzyl (*o*-ClBz), *p* -chlorobenzyl (*p*-ClBz)

Table 3.3.4e
Infrared spectral data for (2-{[1,1-*bis*(hydroxymethyl)-2-oxidoethyl]iminomethyl}-2-methoxy-4-bromophenolato)diorganotin complexes

Complex	*v*(O-H)	*v*(C=N)	*v*(-O-C=N-)	*v*(C-O)	v_a(C-O-C), v_s(C-O-C)	*v*(Sn-O)	*v*(Sn-N)
(2-{[1,1-*Bis*(hydroxymethyl)-2-oxidoethyl]-iminomethyl}-2-methoxy-4-bromophenolato)-dimethyltin(IV), **TE2**	3395b	1611s	1544m	1180m	1071m, 1039m	670w	469w
(2-{[1,1-*Bis*(hydroxymethyl)-2-oxidoethyl]-iminomethyl}-2-methoxy-4-bromophenolato)-dibutyltin(IV), **TE2**	3329b	1608s	1542m	1183m	1060m, 1038m	681m	468w
(2-{[1,1-*Bis*(hydroxymethyl)-2-oxidoethyl]-iminomethyl}-2-methoxy-4-bromophenolato)-diphenyltin(IV), **TE3**	3390b	1611s	1543m	1187m	1074m, 1040m	697w	471w
(2-{[1,1-*Bis*(hydroxymethyl)-2-oxidoethyl]-iminomethyl}-2-methoxy-4-bromophenolato)-dicyclohexyltin(IV), **TE4**	3341b	1607s	1542m	1175m	1071m, 1037m	683w	462w
(2-{[1,1-*Bis*(hydroxymethyl)-2-oxidoethyl]-iminomethyl}-2-methoxy-4-bromophenolato)-dibenzyltin(IV), **TE5**	3343b	1610s	1545m	1178m	1071m, 1038m	685w	464w
(2-{[1,1-*Bis*(hydroxymethyl)-2-oxidoethyl]-iminomethyl}-2-methoxy-4-bromophenolato)-di(*o*-chlorobenzyl)tin(IV), **TE6**	3433b	1617s	1544m	1170m	1086m, 1047m	678w	462w
(2-{[1,1-*Bis*(hydroxymethyl)-2-oxidoethyl]-iminomethyl}-2-methoxy-4-bromophenolato)-di(*p*-chlorobenzyl)tin(IV), **TE7**	3399b	1618s	1580m	1170m	1082m, 1052m	708w	438w

s = strong, m = medium, w = weak, sh = shoulder, b = broad

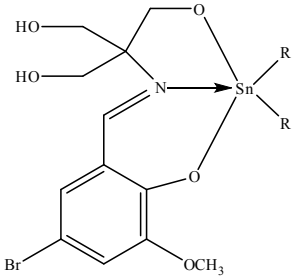

R = CH_3, C_4H_9, phenyl (Ph), cyclohexyl (Cy), benzyl (Bz), *o*-chlorobenzyl (*o*-ClBz), *p*-chlorobenzyl (*p*-ClBz)

3.3.3 NMR Spectral Data

Most of the Schiff base ligands and organotin complexes had poor solubility in common deuterated solvents such as $CDCl_3$, CD_3OD, CD_3CN, $(CD_3)_2CO$ and C_6D_6. Therefore, the ligands and complexes were prepared and dissolved in deuterated DMSO.

^{1}H NMR chemical shifts for ligands are listed in table 3.3.5 while the ^{13}C NMR chemical shifts for ligands are listed in table 3.3.6. The ^{1}H NMR chemical shifts for the complexes are listed in table 3.3.7 and the ^{13}C NMR chemical shifts for complexes are listed in table 3.3.8; while the ^{119}Sn NMR chemical shifts are listed in table 3.3.9.

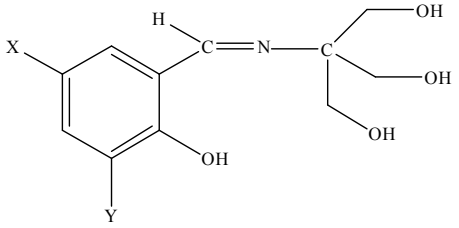

TA: X = H, Y= H ; **TB**: X = Br, Y = H;
TC: X = Cl, Y = H; **TD**: X = NO_2, Y = H;
TE: X= Br, Y = OCH_3

^{1}H NMR Spectra

The presence of a sharp resonance signal in the range of 4.70-5.10 ppm for Schiff base ligands **TA**, **TB**, **TC**, **TD** and **TE** was assigned to the three equivalent hydroxy protons from the hydroxymethyl group. The methine protons of the azomethine group, -N=C(H)- occured as a single peak in the range of 8.30-8.70 ppm for the ligands. The chemical shift for the methylene protons existed as a group of multiplets in the range of 3.30-3.80 ppm while the chemical shift for the phenyl protons was in the range of 6.20-8.00 ppm. The methoxy protons for ligand **TE** occurred as a singlet and could be found at 3.95 ppm and this was in good agreement with those reported in literature [Pavia *et al.,* 2001].

Similarly, in the organotin complexes, the chemical shift for the methylene protons could also be observed as a group of multiplets in the range of 3.00-4.00 ppm while the chemical shift for the aryl protons was in the range of 6.20-8.50 ppm. The HC=N azomethine proton of the diorganotin complexes was observed as a sharp singlet in the region of 8.20-9.00 ppm which varied slightly from those reported for the Schiff base ligands.

In the ^{1}H NMR spectra for the organotin complexes, the presence of a strong signal in the range of 4.70-5.10 ppm indicated the presence of the hydroxy protons from the hydroxymethyl groups. This evidence further supported the fact that not all the hydroxy protons were involved in the coordination to the centre tin atom. The decrease in the integration value of the OH proton signal in the organotin complexes suggested the bonding of the tin atom to one of oxygen atom of the Schiff base ligand through the replacement of one of the phenolic protons.

The chemical shift values of the aromatic and aliphatic protons of the complexes were located in the expected region of the spectra. These chemical shifts information were useful for the confirmation of the presence of the alkyl and aryl groups in the complexes.

^{13}C NMR spectra

The chemical shifts of the azomethine carbon in the ligands **TA**, **TB**, **TC**, **TD** and **TE** occurred in the range of 162-166 ppm. Among the Schiff base ligands, **TD** showed the highest C(7) chemical value at 166.3 ppm. Also the chemical shift value for C(5) in **TD** was the highest, probably due to the presence of the nitro substituent in the aryl ring. Nitro groups are strong electron-withdrawing functional groups which remove electron density from aryl rings. This in turn affects the electron density on the azomethine nitrogen which gave rise to the highest deshielding effect on C(7). The presence of the electron donating groups, Cl and Br, on C(5) did not display result in large shifts in its chemical shift values in the diorganotin complexes in comparison to the Schiff base ligands.

The ^{13}C NMR chemical shift for the quarternary carbon, C(8), was observed between 65-68 ppm in the TRIS Schiff base ligands and the diorganotin complexes. The chemical shift values for the methylene carbons, C(9), C(10) and C(11) can be found in the region of 61-62 for the ligands while for the diorganotin complexes, its chemical shift value range was slightly wider, between 60-70 ppm due to the influence of the interaction between the methylene oxygen and the tin atom. The ^{13}C NMR chemical shift value for the methoxy substituent in ligand **TE** and its complexes was observed at around 56 ppm.

The ^{13}C NMR spectra for the complexes showed a significant downfield shift for all carbon resonances as compared to the free ligands, as a consequence of the electron density transfer from the ligand to the acceptor. The chemical shifts of the aryl carbons were observed between 110-160 ppm and these values were consistent with those of aromatic carbons [Yin and Chen 2006a, Yin and Chen 2006b].

As some of the complexes had poor solubility in most of the deuterated solvent, including DMSO, rigorous assignments of the carbon peaks could not be done especially on the *J*-coupling constants [$^{n}J(^{119}Sn\text{-}^{13}C)$] of the organotin fragments. Also, some of the aryl carbons for the dibenzyltin and substituted dibenzyltin complexes were not observed due to the high signal-to-noise (S/N) overlapping with the carbon signals because of the insolubility of the complexes in deuterated solvents.

^{119}Sn NMR Spectra

^{119}Sn NMR spectroscopy was used as an additional chemical tool to predict the coordination environment of tin in the complexes. From the table, the ^{119}Sn NMR chemical shifts of the dimethyltin complexes were found between -158 to -174 ppm, dibutyltin complexes at around -179 to -190 ppm, diphenyltin complexes at around -325 ppm and dicyclohexyltin complexes at -238 to -283 ppm. These ^{119}Sn NMR chemical shift values were found to be in the similar range to those reported for the respective diorganotin compounds indicating that most of these diorganotin complexes displayed five-coordinate tin geometry.

However, the ^{119}Sn NMR chemical shift values were not obtained for some of the dibenzyltin, di(*o*-chlorobenzyl)tin and di(*p*-chlorobenzyl)tin as the complexes had poor solubility in most deuterated solvents including deuterated DMSO. The ^{119}Sn NMR chemical shifts for some of the dibenzyltins and substituted dibenzyltins showed that their chemical shift values covered over a wide range, from -275 to -520 ppm. One of the reasons that the complexes were not in a five-coordinated coordination could be due to many factors such as the presence of the solvate solvent in the complexes.

Table 3.3.5
^{1}H NMR chemical shifts for the TRIS ligands

Ligand	Assignments[a] [δ(^{1}H)/ppm]			
	Aryl	-N=C(H)	-C-CH_2-, -OCH_3	-OH
2-{[1,1-*Bis*(hydroxymethyl)-2-oxidoethyl]iminomethyl}-phenol, **TA**	6.63-6.73 (m, 3H), 7.13-7.26 (m, 2H)	8.47 (s, 1H)	3.47-3.59 (m, 6H)	4.76 (s, 3H)
2-{[1,1-*Bis*(hydroxymethyl)-2-oxidoethyl]iminomethyl}-4-bromophenol, **TB**	6.67-6.71 (m, 1H), 7.34-7.62 (m, 2H)	8.50 (s, 1H)	3.47-3.59 (m, 6H)	4.85 (s, 3H)
2-{[1,1-*Bis*(hydroxymethyl)-2-oxidoethyl]iminomethyl}-4-chlorophenol, **TC**	6.73-6.76 (m, 1H), 7.25-7.50 (m, 2H)	8.51 (s, 1H)	3.42-3.59 (m, 6H)	4.83 (s, 3H)
2-{[1,1-*Bis*(hydroxymethyl)-2-oxidoethyl]iminomethyl}-4-nitrophenol, **TD**	6.25-6.52 (m, 1H), 7.81-8.54 (m, 2H)	8.70 (s, 1H)	3.50-3.62 (m, 6H)	5.28 (s, 3H)
2-{[1,1-*Bis*(hydroxymethyl)-2-oxidoethyl]iminomethyl}-2-methoxy-4-bromophenol, **TE**	6.83.6.89 (m, 1H), 7.01-7.10 (m, 1H)	8.35 (s, 1H)	3.37-3.75 (m, 6H), 3.95 (s, 3H)	5.06 (s, 3H)

[a] s = singlet, d = doublet, t = triplet, m = multiplet

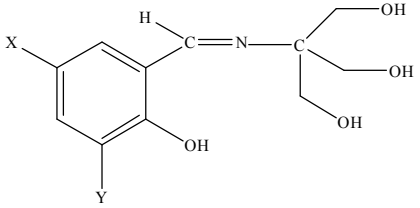

TA: X = H, Y= H ; **TB**: X = Br, Y = H;
TC: X = Cl, Y = H; **TD**: X = NO_2, Y = H;
TE: X= Br, Y = OCH_3

Table 3.3.6a
^{1}H NMR chemical shifts for (2-{[1,1-*bis*(hydroxymethyl)-2-oxidoethyl]iminomethyl}phenolato)diorganotin complexes

Complex	Assignments[a] [δ(^{1}H)/ppm]				
	Aryl	-N=C(H)	-OH	-C-CH$_2$-	R group
(2-{[1,1-*Bis*(hydroxymethyl)-2-oxidoethyl]-iminomethyl}phenolato)dimethyltin(IV), **TA1**	6.59-6.67 (m, 2H), 7.30-7.33 (m, 2H)	8.39 (s, 1H)	5.21 (s, 2H)	3.47-3.60 (m, 6H)	0.43 (s, 6H)
(2-{[1,1-*Bis*(hydroxymethyl)-2-oxidoethyl]-iminomethyl}phenolato)dibutyltin(IV), **TA2**	6.62-6.69 (m, 2H), 7.14-7.37 (m, 2H)	8.94 (s, 1H)	5.24 (s, 2H)	3.55-3.85 (m, 6H)	0.83-2.00 (m, 18H)
(2-{[1,1-*Bis*(hydroxymethyl)-2-oxidoethyl]-iminomethyl}phenolato)diphenyltin(IV), **TA3**	6.69-6.75 (m, 2H), 6.93-8.00 (m, 3H)	8.58 (s, 1H)	5.27 (s, 2H)	3.48-3.93 (m, 6H)	6.93-8.00 (m, 10H)
(2-{[1,1-*Bis*(hydroxymethyl)-2-oxidoethyl]-iminomethyl}phenolato)dicyclohexyltin(IV), **TA4**	6.55-6.57(m, 2H), 7.23-7.27 (m, 2H)	8.39(s, 1H)	5.02 (s, 2H)	3.57-3.70 (m, 6H)	1.24-1.76 (m, 20H), 2.45-2.46 (m, 2H)
(2-{[1,1-*Bis*(hydroxymethyl)-2-oxidoethyl]-iminomethyl}phenolato)dibenzyltin(IV), **TA5**	6.90-7.50 (m, 4H)	8.40 (s,1H)	5.04 (s, 2H)	3.00-3.30 (m, 6H)	1.10-1.23 (m, 4H), 6.90-7.50 (m, 10H)
(2-{[1,1-*Bis*(hydroxymethyl)-2-oxidoethyl]-iminomethyl}phenolato)di(*o*-chlorobenzyl)tin(IV), **TA6**	7.16-7.87 (m, 4H)	8.58 (s, 1H)	5.18 (s, 2H)	3.80-3.86 (m, 6H),	1.11-1.19 (m, 4H), 7.16-7.87 (m, 8H)
(2-{[1,1-*Bis*(hydroxymethyl)-2-oxidoethyl]-iminomethyl}phenolato)di(*p*-chlorobenzyl)tin(IV), **TA7**	6.74-7.66 (m, 4H)	8.56 (s, 1H)	5.20 (s, 2H)	3.69-3.90 (m, 6H)	1.13-1.20 (m, 4H), 6.74-7.66 (m, 8H)

[a] s = singlet, d = doublet, t = triplet, m = multiplet

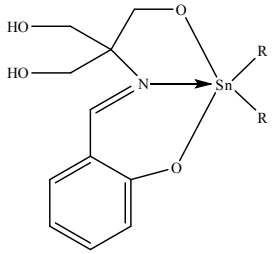

R = CH_3, C_4H_9, phenyl (Ph), cyclohexyl (Cy), benzyl (Bz), *o*-chlorobenzyl (*o*-ClBz), *p* -chlorobenzyl (*p*-ClBz)

Table 3.3.6b
^{1}H NMR chemical shifts for (2-{[1,1-*bis*(hydroxymethyl)-2-oxidoethyl]iminomethyl}-4-bromophenolato)diorganotin complexes

Complex	Assignments[a] [δ(^{1}H)/ppm]				
	Aryl	-N=C(H)	-OH	-C-CH$_2$-	R group
Bis[(2-{[1,1-*Bis*(hydroxymethyl)-2-oxidoethyl]-iminomethyl}-4-bromophenolato)]dimethyltin(IV), **TB1**	6.60-7.40 (m, 3H)	8.85 (s, 1H)	5.30 (s, 2H)	3.69-3.80 (m, 6H)	0.63 (s, 6H)
(2-{[1,1-*Bis*(hydroxymethyl)-2-oxidoethyl]iminomethyl}-4-bromophenolato)dibutyltin(IV), **TB2**	6.60-6.64 (m, 1H), 7.27-7.38 (m, 2H)	8.94 (s, 1H)	5.45 (s, 2H)	3.50-3.85 (m, 6H)	0.85-2.00 (s, 18H)
(2-{[1,1-*Bis*(hydroxymethyl)-2-oxidoethyl]iminomethyl}-4-bromophenolato)diphenyltin(IV), **TB3**	6.90-6.93 (m, 1H), 7.37- 7.76 (m, 2H)	8.52 (s, 1H)	5.04 (s, 2H)	3.56-3.93 (m, 6H)	7.37- 7.76 (m. 10H)
(2-{[1,1-*Bis*(hydroxymethyl)-2-oxidoethyl]iminomethyl}-4-bromophenolato)dicyclohexyltin(IV), **TB4**	6.43-6.75 (m, 1H), 7.09-7.61 (m, 2H)	8.39 (s, 1H)	5.10 (s, 2H)	3.50-3.62 (m, 6H)	1.07-2.25 (m, 22H)
(2-{[1,1-*Bis*(hydroxymethyl)-2-oxidoethyl]iminomethyl}-4-bromophenolato)dibenzyltin(IV), **TB5**	6.60-6.70 (m, 1H), 7.44-7.77 (m, 2H)	8.59 (s, 1H)	5.21 (s, 2H)	3.43-3.68 (m, 6H)	1.12-1.20 (m, 4H), 7.44-7.77 (m, 10H)
(2-{[1,1-*Bis*(hydroxymethyl)-2-oxidoethyl]iminomethyl}-4-bromophenolato)di(*o*-chlorobenzyl)tin(IV), **TB6**	6.43-6.67 (m, 1H), 7.01-7.70 (m, 2H)	8.49 (s, 1H)	5.20 (s, 2H)	3.00-3.48 (m, 6H)	1.12-1.34 (m, 4H), 7.01-7.70 (m, 8H)
(2-{[1,1-*Bis*(hydroxymethyl)-2-oxidoethyl]iminomethyl}-4-bromophenolato)di(*p*-chlorobenzyl)tin(IV), **TB7**	6.44-6.63 (m, 1H), 7.00-7.81 (m, 2H)	8.60 (s, 1H)	5.19 (s, 2H)	3.04-3.72 (m, 6H)	1.13-1.20 (m, 4H), 7.00-7.81 (m, 8H)

[a] s = singlet, d = doublet, t = triplet, m = multiplet

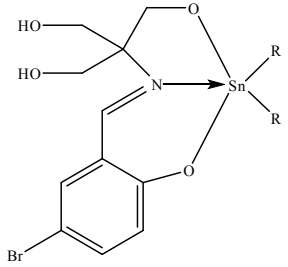

R = CH_3, C_4H_9, phenyl (Ph), cyclohexyl (Cy), benzyl (Bz), *o*-chlorobenzyl (*o*-ClBz), *p*-chlorobenzyl (*p*-ClBz)

Table 3.3.6c
^{1}H NMR chemical shifts for (2-{[1,1-*bis*(hydroxymethyl)-2-oxidoethyl]iminomethyl}-4-chlorophenolato)diorganotin complexes

Complex	Assignments[a] [δ(^{1}H)/ppm]				
	Aryl	-N=C(H)	-OH	-C-CH$_2$-	R group
(2-{[1,1-*Bis*(hydroxymethyl)-2-oxidoethyl]iminomethyl}-4-chlorophenolatodimethyltin(IV), **TC1**	6.57-6.60 (m, 1H), 7.25-7.48 (m, 2H)	8.40 (s, 1H)	5.02 (s, 2H)	3.40-3.62 (m, 6H)	0.42 (s, 6H)
(2-{[1,1-*Bis*(hydroxymethyl)-2-oxidoethyl]iminomethyl}-4-chlorophenolato)dibutyltin(IV), **TC2**	6.64-6.89 (m, 1H), 7.05-7.42 (m, 2H)	8.91 (s, 1H)	5.27 (s, 2H)	3.68-3.82 (m, 6H)	0.84-2.03 (m, 18H)
(2-{[1,1-*Bis*(hydroxymethyl)-2-oxidoethyl]iminomethyl}-4-chlorophenolato)diphenyltin(IV), **TC3**	6.96- 6.98 (m, 1H), 7.35-7.87 (m, 2H)	8.53 (s, 1H)	5.05 (s, 2H)	3.36-3.89 (m, 6H)	7.35-7.87 (m, 10H)
(2-{[1,1-*Bis*(hydroxymethyl)-2-oxidoethyl]iminomethyl}-4-chlorophenolato)dicyclohexyltin(IV), **TC4**	6.71-6.75 (m, 1H), 7.12-7.40 (m, 2H)	8.56 (s, 1H)	5.13 (s, 2H)	3.39-3.73 (m, 6H)	1.07-1.91 (m, 22H)
(2-{[1,1-*Bis*(hydroxymethyl)-2-oxidoethyl]iminomethyl}-4-chlorophenolato)dibenzyltin(IV), **TC5**	6.65-6.77 (m, 1H), 7.00-7.67 (m, 2H)	8.55 (s, 1H)	5.08 (s, 2H)	3.40-3.75 (m, 6H)	1.14 (m, 4H), 7.00-7.67 (m,10H)
(2-{[1,1-*Bis*(hydroxymethyl)-2-oxidoethyl]iminomethyl}-4-chlorophenolato)di(*o*-chlorobenzyl)tin(IV), **TC6**	6.27- 6.45 (m, 1H), 7.05-7.54 (m, 2H)	8.71 (s, 1H)	5.13 (s, 2H)	3.42-3.81 (m, 6H)	1.21-1.27 (m, 4H), 7.05-7.54 (m, 8H)
(2-{[1,1-*Bis*(hydroxymethyl)-2-oxidoethyl]iminomethyl}-4-chlorophenolato)di(*p*-chlorobenzyl)tin(IV), **TC7**	6.29-6.59 (m, 1H), 7.07-7.57 (m, 2H)	8.60 (s, 1H)	5.14 (s, 2H)	3.50-3.92 (m, 6H)	1.13-1.19 (m, 4H), 7.07-7.57 (m, 8H)

[a] s = singlet, d = doublet, t = triplet, m = multiplet

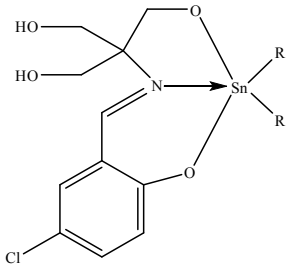

R = CH_3, C_4H_9, phenyl (Ph), cyclohexyl (Cy), benzyl (Bz), *o*-chlorobenzyl (*o*-ClBz), *p*-chlorobenzyl (*p*-ClBz)

Table 3.3.6d
^{1}H NMR chemical shifts for (2-{[1,1-*bis*(hydroxymethyl)-2-oxidoethyl]iminomethyl}-4-nitrophenolato)diorganotin complexes

Complex	Assignments[a] [δ(^{1}H)/ppm]				
	Aryl	-N=C(H)	-OH	-C-CH$_2$-	R group
(2-{[1,1-*Bis*(hydroxymethyl)-2-oxidoethyl]iminomethyl}-4-nitrophenolato)dimethyltin(IV), **TD1**	6.22-6.37 (m, 1H), 7.46-7.99 (m, 2H)	8.22 (s, 1H)	5.02 (s, 2H)	3.13-3.70 (m, 6H)	0.29 (s, 6H)
(2-{[1,1-*Bis*(hydroxymethyl)-2-oxidoethyl]iminomethyl}-4-nitrophenolato)dibutyltin(IV), **TD2**	6.51-6.55 (m, 1H), 7.94-8.25 (m, 2H)	8.65 (s, 1H)	5.10 (s, 2H)	3.07-3.68 (m, 6H)	0.76-1.48 (m, 18H)
(2-{[1,1-*Bis*(hydroxymethyl)-2-oxidoethyl]iminomethyl}-4-nitrophenolato)diphenyltin(IV), **TD3**	7.12-7.68 (m, 10H), 8.40-8.44 (m, 2H)	8.58 (s, 1H)	5.01 (s, 2H)	3.07-3.64 (m, 6H)	7.12-7.68 (m, 10H)
(2-{[1,1-*Bis*(hydroxymethyl)-2-oxidoethyl]iminomethyl}-4-nitrophenolato)dicyclohexyltin(IV), **TD4**	6.66-6.69 (m, 1H), 8.07-8.51 (m, 2H)	8.62 (s, 1H)	5.07 (s, 2H)	3.37-3.80 (m, 6H)	1.25-1.98 (m, 22H)
(2-{[1,1-*Bis*(hydroxymethyl)-2-oxidoethyl]iminomethyl}-4-nitrophenolato)dibenzyltin(IV), **TD5**	6.46-6.50 (m, 1H), 6.91-7.10 (m, 2H)	8.49 (s, 1H)	5.08 (s, 2H)	3.03-3.65 (m, 6H)	1.12-1.15 (m, 4H), 6.91-7.10 (m, 10H)
(2-{[1,1-*Bis*(hydroxymethyl)-2-oxidoethyl]iminomethyl}-4-nitrophenolato)di(*o*-chlorobenzyl)tin(IV), **TD6**	6.19-6.22 (m, 1H) 6.86-7.62 (m, 2H)	8.52 (s, 1H)	5.14 (s, 2H)	3.00-3.27 (m, 6H)	1.14-1.19 m, 4H), 6.86-7.62 (m, 8H)
(2-{[1,1-*Bis*(hydroxymethyl)-2-oxidoethyl]iminomethyl}-4-nitrophenolato)di(*p*-chlorobenzyl)tin(IV), **TD7**	6.48-6.69 (m, 1H), 7.06-7.98 (m, 2H)	8.55 (s, 1H)	5.31 (s, 2H)	3.07-3.63 (m, 6H)	1.15-1.24 (m, 4H), 7.06-7.98 (m, 8H)

[a] s = singlet, d = doublet, t = triplet, m = multiplet

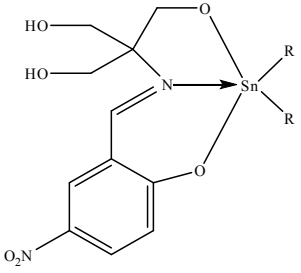

R = CH_3, C_4H_9, phenyl (Ph), cyclohexyl (Cy), benzyl (Bz), *o*-chlorobenzyl (*o*-ClBz), *p* -chlorobenzyl (*p*-ClBz)

Table 3.3.6e
^{1}H NMR chemical shifts for (2-{[1,1-*bis*(hydroxymethyl)-2-oxidoethyl]iminomethyl}-2-methoxy-4-bromophenolato)diorganotin complexes

Complex	Assignments[a] [δ(^{1}H)/ppm]				
	Aryl	-N=C(H)	-OH	-C-CH_2- and -O-CH_3	R group
(2-{[1,1-*Bis*(hydroxymethyl)-2-oxidoethyl]iminomethyl}-2-methoxy-4-bromophenolato)dimethyltin(IV), **TE1**	6.93-6.95 (m, 1H), 7.10-7.13 (m, 1H)	8.82 (s, 1H)	5.10 (s, 2H)	3.70-3.80 (6H), 3.88 (s, 3H)	0.69 (s, 6H)
(2-{[1,1-*Bis*(hydroxymethyl)-2-oxidoethyl]iminomethyl}-2-methoxy-4-bromophenolato)dibutyltin(IV), **TE2**	6.97-6.98 (m, 1H), 7.15-7.18 (m, 1H)	8.38 (s, 1H)	5.02 (s, 2H)	3.45-3.70 (6H), 3.73 (s, 3H)	0.76-1.54 (m, 18H)
(2-{[1,1-*Bis*(hydroxymethyl)-2-oxidoethyl]iminomethyl}-2-methoxy-4-bromophenolato)diphenyltin(IV), **TE3**	6.95-7.03 (m, 1H), 7.15-7.26 (m, 1H)	8.87 (s, 1H)	5.20 (s, 2H)	3.74-3.94 (m, 6H), 3.96 (s, 3H)	7.37-7.88 (m, 10H)
(2-{[1,1-*Bis*(hydroxymethyl)-2-oxidoethyl]iminomethyl}-2-methoxy-4-bromophenolato)dicyclohexyltin(IV), **TE4**	6.53-6.55 (m, 1H), 6.91-7.09 (m, 1H)	8.34 (s, 1H)	5.11 (s, 2H)	3.60-3.68 (m, 6H), 3.95 (s, 3H)	1.00-2.26 (m, 22H)
(2-{[1,1-*Bis*(hydroxymethyl)-2-oxidoethyl]iminomethyl}-2-methoxy-4-bromophenolato)dibenzyltin(IV), **TE5**	6.90-7.89 (m, 2H)	8.69 (s, 1H)	5.23 (s, 2H)	3.56-3.82 (m, 6H), 3.90 (s, 3H)	1.12-1.19 (m, 4H) 6.90-7.89 (m, 10H)
(2-{[1,1-*Bis*(hydroxymethyl)-2-oxidoethyl]iminomethyl}-2-methoxy-4-bromophenolato)di(*o*-chlorobenzyl)tin(IV), **TE6**	6.82-7.59 (m, 2H)	8.90 (s, 1H)	5.22 (s, 2H)	3.50-3.86 (m, 6H), 3.93 (s, 3H)	1.13-1.18 (m, 4H), 6.22-7.59 (m, 8H)
(2-{[1,1-*Bis*(hydroxymethyl)-2-oxidoethyl]iminomethyl}-2-methoxy-4-bromophenolato)di(*p*-chlorobenzyl)tin(IV), **TE7**	6.85-7.50 (m, 2H)	8.99 (s, 1H)	5.12 (s, 2H)	3.45-3.89 (m, 6H), 3.92 (s, 3H)	1.25-1.31 (m, 4H), 6.33-7.50 (m, 8H)

[a] s = singlet, d = doublet, t = triplet, m = multiplet

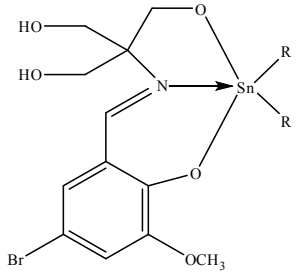

R = CH_3, C_4H_9, phenyl (Ph), cyclohexyl (Cy), benzyl (Bz), *o*-chlorobenzyl (*o*-ClBz), *p*-chlorobenzyl (*p* -ClBz)

Table 3.3.7
^{13}C NMR chemical shifts for the TRIS ligands

Ligand	^{13}C NMR chemical shifts [$\delta(^{13}C)$/ppm]
2-{[1,1-*Bis*(hydroxymethyl)-2-oxidoethyl]-iminomethyl}phenol, **TA**	61.5 ($C_{aliphatic}$), 67.2 (C_8), 117.3 (C_3), 117.7 (C_1), 118.6 (C_5), 132.4 (C_6), 132.6 (C_4), 163.7 (C_2), 164.6 (C_7)
2-{[1,1-*Bis*(hydroxymethyl)-2-oxidoethyl]-iminomethyl}-4-bromophenol, **TB**	61.2 ($C_{aliphatic}$), 67.2 (C_8), 118.8 (C_5), 119.6 (C_3), 120.4 (C_1), 131.3 (C_6), 132.7 (C_4), 163.8 (C_2), 164.3 (C_7)
2-{[1,1-*Bis*(hydroxymethyl)-2-oxidoethyl]-iminomethyl}-4-chlorophenol, **TC**	61.2 ($C_{aliphatic}$), 67.2 (C_8), 106.6 (C_5), 119.4 (C_3), 121.1 (C_1), 134.4 (C_6), 135.5 (C_4), 163.8 (C_2), 165.1 (C_7)
2-{[1,1-*Bis*(hydroxymethyl)-2-oxidoethyl]-iminomethyl}-4-nitrophenol, **TD**	61.0 ($C_{aliphatic}$), 66.6 (C_8), 113.2 (C_3), 123.7(C_1), 129.6 (C_5), 132.9 (C_6), 134.0 (C_4), 166.3 (C_2), 179.9 (C_7)
2-{[1,1-*Bis*(hydroxymethyl)-2-oxidoethyl]-iminomethyl}-2-methoxy-4-bromophenol, **TE**	56.7 ($O\underline{C}H_3$), 61.0 ($C_{aliphatic}$), 66.6 (C_8), 103.2 (C_5), 116.4 (C_3), 126.0 (C_1), 132.9 (C_6), 134.0 (C_4), 163.0 (C_2), 163.3 (C_7)

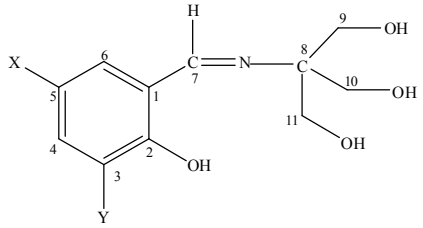

TA: X = H, Y= H ; **TB**: X = Br, Y = H;
TC: X = Cl, Y = H; **TD**: X = NO_2, Y = H;
TE: X= Br, Y = OCH_3

Table 3.3.8a
^{13}C NMR chemical shifts for (2-{[1,1-*bis*(hydroxymethyl)-2-oxidoethyl]iminomethyl}phenolato)diorganotin complexes

Complex	^{13}C NMR chemical shifts [δ(^{13}C)/ppm]
(2-{[1,1-*Bis*(hydroxymethyl)-2-oxidoethyl]-iminomethyl}phenolato)dimethyltin(IV), **TA1**	1.1 [^{1}J(^{119}Sn-^{13}C) = 678 Hz] δ(Sn-Me), 61.5, 62.4 ($C_{aliphatic}$), 67.3 (C_8), 117.8, 118.5, 121.9, 133.5, 136.5, 168.4, 173.3 (C_7)
(2-{[1,1-*Bis*(hydroxymethyl)-2-oxidoethyl]-iminomethyl}phenolato)dibutyltin(IV), **TA2**	13.6, 21.2 [^{1}J(^{119}Sn-^{13}C) = 627 Hz], 26.8 [^{3}J(^{119}Sn-^{13}C) = 80 Hz], 27.3 [^{2}J(^{119}Sn-^{13}C) = 33 Hz] δ(Sn-Bu), 63.7, 64.2 ($C_{aliphatic}$), 66.9 (C_8), 116.1, 117.6, 122.3, 135.9, 136.7, 169.7, 173.6 (C_7)
(2-{[1,1-*Bis*(hydroxymethyl)-2-oxidoethyl]-iminomethyl}phenolato)diphenyltin(IV), **TA3**	59.3, 61.5 ($C_{aliphatic}$), 67.9 (C_8), 116.6, 117.7, 122.0, 127.2, 127.8 [^{3}J(^{119}Sn-^{13}C) = 91 Hz], 128.3, 130.0, 135.0, 136.5 [^{2}J(^{119}Sn-^{13}C) = 22 Hz], 136.7, 141.8 [^{1}J(^{119}Sn-^{13}C) = 697 Hz], 168.8, 173.7 (C_7)
(2-{[1,1-*Bis*(hydroxymethyl)-2-oxidoethyl]-iminomethyl}phenolato)dicyclohexyltin(IV), **TA4**	26.4, 28.8 [^{3}J(^{119}Sn-^{13}C) = 90 Hz], 30.4 [^{2}J(^{119}Sn-^{13}C) = 36 Hz], 39.4 [^{1}J(^{119}Sn-^{13}C) = 590 Hz] δ(Sn-Cyh), 60.4, 61.8 ($C_{aliphatic}$), 67.5 (C_8), 115.6, 118.0, 122.0, 136.2, 136.7, 170.1, 173.4 (C_7)
(2-{[1,1-*Bis*(hydroxymethyl)-2-oxidoethyl]-iminomethyl}phenolato)dibenzyltin(IV), **TA5**	10.8 [^{1}J(^{119}Sn-^{13}C) = 676 Hz] δ(Sn-CH_2), 61.4, 63.2($C_{aliphatic}$), 67.0 (C_8), 116.8, 117.2, 117.6, 118.2, 122.0, 128.2, 132.3, 132.6, 135.7, 136.4, 163.7, 164.6, 172.3 (C_7)
(2-{[1,1-*Bis*(hydroxymethyl)-2-oxidoethyl]-iminomethyl}phenolato)di(*o*-chlorobenzyl)tin(IV), **TA6**	9.0 [^{1}J(^{119}Sn-^{13}C) = 616 Hz] δ(Sn-CH_2), 61.8, 63.0 ($C_{aliphatic}$), 65.2 (C_8), 115.1, 125.9, 126.6, 127.0, 128.9, 129.7, 130.6, 131.7, 133.3, 134.2, 138.2, 169.1, 173.7 (C_7)
(2-{[1,1-*Bis*(hydroxymethyl)-2-oxidoethyl]-iminomethyl}phenolato)di(*p*-chlorobenzyl)tin(IV), **TA7**	8.9 [^{1}J(^{119}Sn-^{13}C) = 624 Hz] δ(Sn-CH_2), 61.7, 62.5 ($C_{aliphatic}$), 66.3 (C_8), 117.3, 126.0, 127.5, 128.5, 129.5, 129.9, 130.7, 131.0, 133.6, 135.2, 138.0, 167.3, 172.2 (C_7)

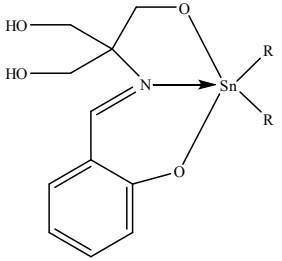

R = CH_3, C_4H_9, phenyl (Ph), cyclohexyl (Cy), benzyl (Bz), *o*-chlorobenzyl (*o*-ClBz), *p*-chlorobenzyl (*p*-ClBz)

Table 3.3.8b
^{13}C NMR chemical shifts for (2-{[1,1-*bis*(hydroxymethyl)-2-oxidoethyl]iminomethyl}-4-bromophenolato)diorganotin complexes

Complex	^{13}C NMR chemical shifts [δ(^{13}C)/ppm]
Bis[(2-{[1,1-*Bis*(hydroxymethyl)-2-oxidoethyl]-iminomethyl}-4-bromophenolato)]dimethyltin(IV), **TB1**	12.2 [^{1}J(^{119}Sn-^{13}C) = 585 Hz δ(Sn-Me), 63.8, 64.4 ($C_{aliphatic}$), 67.0 (C_8), 106.6, 114.9, 124.3, 132.0, 136.9, 158.8 (C_2), 172.0 (C_7)
(2-{[1,1-*Bis*(hydroxymethyl)-2-oxidoethyl]-iminomethyl}-4-bromophenolato)dibutyltin(IV), **TB2**	13.6, 21.3 [^{1}J(^{119}Sn-^{13}C) = 604 Hz], 26.8 [^{3}J(^{119}Sn-^{13}C) = 82 Hz], 27.3 [^{2}J(^{119}Sn-^{13}C) = 36 Hz] δ(Sn-Bu), 62.4, 63.6 ($C_{aliphatic}$), 67.3 (C_8), 106.8, 118.8, 124.4, 137.2, 139.1, 168.5 (C_2), 172.9 (C_7)
(2-{[1,1-*Bis*(hydroxymethyl)-2-oxidoethyl]-iminomethyl}-4-bromophenolato)diphenyltin(IV), **TB3**	61.1 64.0($C_{aliphatic}$), 68.3 (C_8), 106.4, 119.3, 124.5, 128.7 [^{3}J(^{119}Sn-^{13}C) = 90 Hz], 129.6, 130.0, 135.0, 136.3 [^{2}J(^{119}Sn-^{13}C) = 27 Hz], 137.7, 138.4 [^{1}J(^{119}Sn-^{13}C) = 711 Hz], 141.9, 167.7 (C_2), 172.7 (C_7)
(2-{[1,1-*Bis*(hydroxymethyl)-2-oxidoethyl]-iminomethyl}-4-bromophenolato)dicyclohexyltin(IV), **TB4**	26.4, 28.1 [^{3}J(^{119}Sn-^{13}C) = 82 Hz], 29.9 [^{2}J(^{119}Sn-^{13}C) = 24 Hz], 37.9 [^{1}J(^{119}Sn-^{13}C) = 658 Hz] δ(Sn-Cyh), 61.0, 61.2 ($C_{aliphatic}$), 67.0 (C_8), 106.5, 119.1, 124.0, 135.2, 137.4, 168.6 (C_2), 172.1 (C_7)
(2-{[1,1-*Bis*(hydroxymethyl)-2-oxidoethyl]-iminomethyl}-4-bromophenolato)dibenzyltin(IV), **TB5**	9.3 [^{1}J(^{119}Sn-^{13}C) = 604 Hz] δ(Sn-CH_2), 60.8, 61.9 ($C_{aliphatic}$), 67.5 (C_8), 106.9, 119.7, 124.0, 124.3, 128.6, 129.0, 130.5, 136.3, 137.5, 138.6, 160.0, 165.8 (C_2), 171.5 (C_7)
(2-{[1,1-*Bis*(hydroxymethyl)-2-oxidoethyl]-iminomethyl}-4-bromophenolato)-di(*o*-chlorobenzyl)tin(IV), **TB6**	8.6 [^{1}J(^{119}Sn-^{13}C) = 708 Hz] δ(Sn-CH_2), 59.3, 60.2 ($C_{aliphatic}$), 68.1 (C_8), 110.8, 120.0, 124.1, 127.1, 128.1, 128.5, 128.8, 129.3, 130.5, 130.9, 138.6, 162.4 (C_2), 169.8 (C_7)
(2-{[1,1-*Bis*(hydroxymethyl)-2-oxidoethyl]-iminomethyl}-4-bromophenolato)-di(*p*-chlorobenzyl)tin(IV), **TB7**	8.7 [^{1}J(^{119}Sn-^{13}C) = 616 Hz] δ(Sn-CH_2), 59.3, 61.0 ($C_{aliphatic}$), 66.4 (C_8), 109.5, 120.0, 124.5, 127.0, 128.1, 128.3, 128.8, 129.4, 130.5, 131.3, 137.6, 165.8 (C_2), 169.7 (C_7)

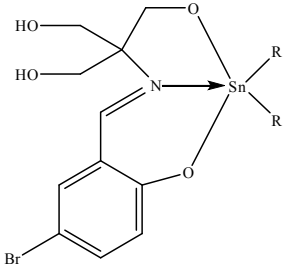

R = CH_3, C_4H_9, phenyl (Ph), cyclohexyl (Cy), benzyl (Bz), *o*-chlorobenzyl (*o*-ClBz), *p*-chlorobenzyl (*p*-ClBz)

Table 3.3.8c
^{13}C NMR chemical shifts for (2-{[1,1-*bis*(hydroxymethyl)-2-oxidoethyl]iminomethyl}-4-chlorophenolato)diorganotin complexes

Complex	^{13}C NMR chemical shifts [δ(^{13}C)/ppm]
(2-{[1,1-*Bis*(hydroxymethyl)-2-oxidoethyl]-iminomethyl}-4-chlorophenolato)dimethyltin(IV), **TC1**	8.7 [^{1}J(^{119}Sn-^{13}C) = 557 Hz] δ(Sn-Me), 61.0, 61.2 ($C_{aliphatic}$), 68.0 (C_8), 118.1, 118.5, 123.8, 134.5, 135.2, 167.1 (C_2), 171.9 (C_7)
(2-{[1,1-*Bis*(hydroxymethyl)-2-oxidoethyl]-iminomethyl}-4-chlorophenolato)dibutyltin(IV), **TC2**	13.6, 21.4 [^{1}J(^{119}Sn-^{13}C) = 611 Hz], 26.9 [^{3}J(^{119}Sn-^{13}C) = 82 Hz], 27.4 [^{2}J(^{119}Sn-^{13}C) = 36 Hz] δ(Sn-Bu), 61.1, 63.8 ($C_{aliphatic}$), 67.3 (C_8), 118.9, 120.3, 124.1, 134.1, 136.6, 168.1 (C_2), 173.0 (C_7)
(2-{[1,1-*Bis*(hydroxymethyl)-2-oxidoethyl]-iminomethyl}-4-chlorophenolato)diphenyltin(IV), **TC3**	61.0, 64.3 ($C_{aliphatic}$), 68.1 (C_8), 118.3, 119.2, 123.9, 128.2 [^{3}J(^{119}Sn-^{13}C) = 79 Hz], 129.0, 129.8, 134.5, 135.6 [^{2}J(^{119}Sn-^{13}C) = 22 Hz], 136.2 [^{1}J(^{119}Sn-^{13}C) = 681 Hz], 136.4, 141.8, 167.3 (C_2), 172.6 (C_7)
(2-{[1,1-*Bis*(hydroxymethyl)-2-oxidoethyl]-iminomethyl}-4-chlorophenolato)dicyclohexyltin(IV), **TC4**	24.2, 28.8 [^{3}J(^{119}Sn-^{13}C) = 72 Hz], 30.2 [^{2}J(^{119}Sn-^{13}C) = 25 Hz], 40.4 [^{1}J(^{119}Sn-^{13}C) = 634 Hz] δ(Sn-Cyh), 60.7, 61.5($C_{aliphatic}$), 68.0 (C_8), 118.5, 121.0, 123.8, 129.3, 134.6, 165.4 (C_2), 168.6 (C_7)
(2-{[1,1-*Bis*(hydroxymethyl)-2-oxidoethyl]-iminomethyl}-4-chlorophenolato)dibenzyltin(IV), **TC5**	9.0 [^{1}J(^{119}Sn-^{13}C) = 610 Hz] δ(Sn-CH_2), 61.4, 63.4 ($C_{aliphatic}$), 67.4 (C_8), 118.9, 119.6, 121.2, 123.8, 124.3, 127.0, 128.2, 129.1, 130.0, 133.4, 142.7, 164.2 (C_2), 167.7 (C_7)
(2-{[1,1-*Bis*(hydroxymethyl)-2-oxidoethyl]-iminomethyl}-4-chlorophenolato)-di(*o*-chlorobenzyl)tin(IV), **TC6**	8.5 [^{1}J(^{119}Sn-^{13}C) = 560 Hz] δ(Sn-CH_2), 60.9, 62.8 ($C_{aliphatic}$), 68.0 (C_8), 116.2, 118.0, 121.8, 124.3, 126.3, 128.9 [^{2}J(^{119}Sn-^{13}C) = 73 Hz], 130.9, 132.3, 135.8, 136.1, 138.4, 168.8 (C_2), 173.3 (C_7)
(2-{[1,1-*Bis*(hydroxymethyl)-2-oxidoethyl]-iminomethyl}-4-chlorophenolato)-di(*p*-chlorobenzyl)tin(IV), **TC7**	8.6 [^{1}J(^{119}Sn-^{13}C) = 693 Hz] δ(Sn-CH_2), 61.3, 62.2 ($C_{aliphatic}$), 67.6 (C_8), 120.0, 124.0, 127.5, 128.2, 128.9 [^{2}J(^{119}Sn-^{13}C) = 86 Hz], 130.6, 131.3, 132.8, 134.7, 135.2, 135.9, 165.5 (C_2), 171.7 (C_7)

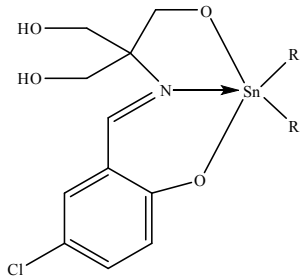

R = CH_3, C_4H_9, phenyl (Ph), cyclohexyl (Cy), benzyl (Bz), *o*-chlorobenzyl (*o*-ClBz), *p*-chlorobenzyl (*p*-ClBz)

Table 3.3.8d
^{13}C NMR chemical shifts for (2-{[1,1-*bis*(hydroxymethyl)-2-oxidoethyl]iminomethyl}-4-nitrophenolato)diorganotin complexes

Complex	^{13}C NMR chemical shifts [δ(^{13}C)/ppm]
(2-{[1,1-*Bis*(hydroxymethyl)-2-oxidoethyl]-iminomethyl}-4-nitrophenolato)dimethyltin(IV), **TD1**	8.8 [^{1}J(^{119}Sn-^{13}C) = 515 Hz] δ(Sn-Me), 59.5, 61.4 ($C_{aliphatic}$), 66.9 (C_8), 113.3, 123.8, 129.8, 133.1, 134.2, 166.5 (C_2), 180.0 (C_7)
(2-{[1,1-*Bis*(hydroxymethyl)-2-oxidoethyl]-iminomethyl}-4-nitrophenolato)dibutyltin(IV), **TD2**	13.4, 21.8 [^{1}J(^{119}Sn-^{13}C) = 665 Hz], 26.5 [^{3}J(^{119}Sn-^{13}C) = 81 Hz], 27.8 [^{2}J(^{119}Sn-^{13}C) = 38 Hz] δ(Sn-Bu), 60.7, 61.7 ($C_{aliphatic}$), 67.2 (C_8), 113.6, 124.3, 130.4, 133.7, 134.5, 166.9 (C_2), 180.5 (C_7)
(2-{[1,1-*Bis*(hydroxymethyl)-2-oxidoethyl]-iminomethyl}-4-nitrophenolato)diphenyltin(IV), **TD3**	60.3, 61.4 ($C_{aliphatic}$), 66.7 (C_8), 113.3, 116.8, 123.2, 127.5, 128.9 [^{3}J(^{119}Sn-^{13}C) = 73 Hz], 130.0, 133.0 [^{2}J(^{119}Sn-^{13}C) = 30 Hz], 134.2, 136.3 [^{1}J(^{119}Sn-^{13}C) = 751 Hz], 136.9, 141.9, 166.5 (C_2), 180.0 (C_7)
(2-{[1,1-*Bis*(hydroxymethyl)-2-oxidoethyl]-iminomethyl}-4-nitrophenolato)dicyclohexyltin(IV), **TD4**	26.4, 28.2 [^{3}J(^{119}Sn-^{13}C) = 74 Hz], 29.9 [^{2}J(^{119}Sn-^{13}C) = 36 Hz], 38.6 [^{1}J(^{119}Sn-^{13}C) = 730 Hz] δ(Sn-Cyh), 63.2, 64.7 ($C_{aliphatic}$), 67.5 (C_8), 116.5, 122.5, 130.0, 134.0, 135.7, 167.8 (C_2), 174.8 (C_7)
(2-{[1,1-*Bis*(hydroxymethyl)-2-oxidoethyl]-iminomethyl}-4-nitrophenolato)dibenzyltin(IV), **TD5**	9.1 [^{1}J(^{119}Sn-^{13}C) = 524 Hz] δ(Sn-CH_2), 60.6, 61.2 ($C_{aliphatic}$), 67.0 (C_8), 113.5, 116.5, 124.2, 124.3, 128.3, 128.4, 128.8, 130.0, 133.3, 134.4, 136.9, 166.7 (C_2), 174.6 (C_7)
(2-{[1,1-*Bis*(hydroxymethyl)-2-oxidoethyl]-iminomethyl}-4-nitrophenolato)-di(*o*-chlorobenzyl)tin(IV), **TD6**	8.7 [^{1}J(^{119}Sn-^{13}C) = 564 Hz] δ(Sn-CH_2), 60.3, 61.2 ($C_{aliphatic}$), 67.9 (C_8), 113.3, 116.7, 122.2, 123.8, 126.0, 128.0, 129.7, 130.6, 132.1, 133.0, 134.1, 166.4 (C_2), 180.0 (C_7)
(2-{[1,1-*Bis*(hydroxymethyl)-2-oxidoethyl]-iminomethyl}-4-nitrophenolato)-di(*p*-chlorobenzyl)tin(IV), **TD7**	8.6 [^{1}J(^{119}Sn-^{13}C) = 564 Hz] δ(Sn-CH_2), 59.3, 60.1 ($C_{aliphatic}$), 66.7 (C_8), 113.2, 123.1, 123.8, 127.2, 127.6, 128.1, 128.8, 129.6, 130.8, 131.2, 134.1, 166.4 (C_2), 180.0 (C_7)

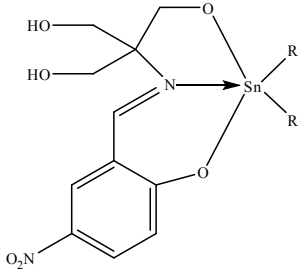

R = CH_3, C_4H_9, phenyl (Ph), cyclohexyl (Cy), benzyl (Bz), *o*-chlorobenzyl (*o*-ClBz), *p*-chlorobenzyl (*p*-ClBz)

Table 3.3.8e
^{13}C NMR chemical shifts for (2-{[1,1-*bis*(hydroxymethyl)-2-oxidoethyl]iminomethyl}-2-methoxy-4-bromophenolato)diorganotin complexes

Complex	^{13}C NMR chemical shifts [δ(^{13}C)/ppm]
(2-{[1,1-*Bis*(hydroxymethyl)-2-oxidoethyl]-iminomethyl}-2-methoxy-4-bromophenolato)-dimethyltin(IV), **TE2**	0.8 [^{1}J(^{119}Sn-^{13}C) = 665 Hz] δ(Sn-Me), 56.3 (-O$\underline{C}$H$_3$), 63.2, 64.3, ($C_{aliphatic}$), 67.5 (C_8), 106.3, 118.0, 128.2, 136.2, 152.3, 163.5 (C_2), 172.6 (C_7)
(2-{[1,1-*Bis*(hydroxymethyl)-2-oxidoethyl]-iminomethyl}-2-methoxy-4-bromophenolato)-dibutyltin(IV), **TE2**	13.7, 21.0 [^{1}J(^{119}Sn-^{13}C) = 627 Hz], 26.8 [^{3}J(^{119}Sn-^{13}C) = 10 Hz], 27.0 [^{2}J(^{119}Sn-^{13}C) = 36 Hz] δ(Sn-Bu), 56.2 (-O$\underline{C}$H$_3$), 61.2, 65.0 ($C_{aliphatic}$), 67.8 (C_8), 104.1, 117.9, 118.3, 128.4, 152.3, 163.6 (C_2), 172.1 (C_7)
(2-{[1,1-*Bis*(hydroxymethyl)-2-oxidoethyl]-iminomethyl}-2-methoxy-4-bromophenolato)-diphenyltin(IV), **TE3**	56.6 (O$\underline{C}$H$_3$), 61.0, 63.2 ($C_{aliphatic}$), 67.9 (C_8), 104.5, 118.2, 125.3, 128.2, 128.7 [^{3}J(^{119}Sn-^{13}C) = 71 Hz], 129.0, 130.1, 133.0[^{2}J(^{119}Sn-^{13}C) = 32 Hz], 136.4 [^{1}J(^{119}Sn-^{13}C) = 682 Hz], 137.2, 139.9, 162.1 (C_2), 175.0 (C_7)
(2-{[1,1-*Bis*(hydroxymethyl)-2-oxidoethyl]-iminomethyl}-2-methoxy-4-bromophenolato)-dicyclohexyltin(IV), **TE4**	26.7, 28.3 [^{3}J(^{119}Sn-^{13}C) = 73 Hz], 30.2 [^{2}J(^{119}Sn-^{13}C) = 33 Hz], 38.6 [^{1}J(^{119}Sn-^{13}C) = 652 Hz] δ(Sn-Cyh), 56.1 (O$\underline{C}$H$_3$), 61.0, 63.4 ($C_{aliphatic}$), 66.3 (C_8), 103.2, 116.3, 126.1, 136.5, 152.3, 163.5 (C_2), 172.9 (C_7)
(2-{[1,1-*Bis*(hydroxymethyl)-2-oxidoethyl]-iminomethyl}-2-methoxy-4-bromophenolato)-dibenzyltin(IV), **TE5**	9.0 [^{1}J(^{119}Sn-^{13}C) = 663 Hz] δ(Sn-CH$_2$), 57.1 (O$\underline{C}$H$_3$), 60.9, 61.5 ($C_{aliphatic}$), 66.5 (C_8), 104.9, 105.1, 110.8, 111.0, 120.1, 121.8, 127.0, 128.6, 129.4, 136.5, 154.4, 163.0 (C_2), 170.9 (C_7)
(2-{[1,1-*Bis*(hydroxymethyl)-2-oxidoethyl]-iminomethyl}-2-methoxy-4-bromophenolato)-di(*o*-chlorobenzyl)tin(IV), **TE6**	8.8 [^{1}J(^{119}Sn-^{13}C) = 586 Hz] δ(Sn-CH$_2$), 56.4 (O$\underline{C}$H$_3$), 62.3, 63.7 ($C_{aliphatic}$), 66.9 (C_8), 112.0, 119.9, 121.5, 124.3, 127.2, 128.8, 132.9, 136.2, 138.6, 148.6, 151.2, 163.5 (C_2), 170.8 (C_7)
(2-{[1,1-*Bis*(hydroxymethyl)-2-oxidoethyl]-iminomethyl}-2-methoxy-4-bromophenolato)-di(*p*-chlorobenzyl)tin(IV), **TE7**	8.5 [^{1}J(^{119}Sn-^{13}C) = 564 Hz] δ(Sn-CH$_2$), 56.1 (O$\underline{C}$H$_3$), 61.9, 63.4 ($C_{aliphatic}$), 67.9 (C_8), 111.0, 120.4, 121.8, 125.1, 127.9, 128.2, 132.3, 136.5, 140.6, 149.2, 150.6, 163.2 (C_2),170.3 (C_7)

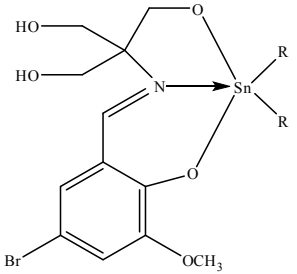

R = CH_3, C_4H_9, phenyl (Ph), cyclohexyl (Cy), benzyl (Bz), *o*-chlorobenzyl (*o*-ClBz), *p*-chlorobenzyl (*p*-ClBz)

Table 3.3.9
^{119}Sn NMR chemical shifts of TRIS diorganotin complexes

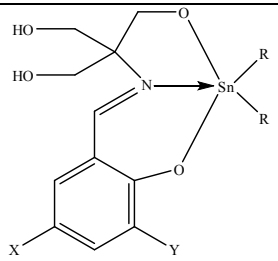	^{119}Sn NMR chemical shifts [δ(^{119}Sn)/ppm]						
	R = Me	R = Bu	R = Ph	R = Cy	R = Bz	R = *o*-ClBz	R = *p*-ClBz
TA: X = H, Y = H	-164.4	-189.2	-324.7	-244.5	-	-	-
TB: X = Br, Y = H	-174.8	-186.9	-325.5	-243.1	-460.0	-459.3	-506.7
TC: X = Cl, Y = H	-163.4	-186.6	-325.3	-244.2	--	-261.9	-
TD: X = NO_2, Y = H	-164.1	-179.2	-330.2	-238.5	-279.1	-271.9	-408.3
TE: X = Br, Y = OCH_3	-158.0	-179.0	-318.6	-283.0	-514.2	-450.8	-

3.3.4 Electronic Spectra

The electronic spectral data of the Schiff base ligands and organotin complexes in acetonitrile (CH_3CN) were recorded in the 190-600 nm regions. Due to the poor solubility of some of the complexes in CH_3CN and most solvents, only selected UV spectra were recorded. Selected spectral data for the TRIS Schiff base ligands **TA**, **TB**, **TC**, **TD** and **TE** and its diorganotin complexes are given in table 3.3.10 and table 3.3.11 respectively.

The absorption bands of the free TRIS Schiff base ligands could be classified into two absorption regions of 200-260 nm and 310-350 nm. However, there was a large shift in the absorption bands of the **TA**, **TB**, **TC** and **TD** complexes; between 190-249 nm and 250-400 nm. For the **TE** complexes, the absorption bands were found between the 190-220 nm and 221-350 nm.

The $n \longrightarrow \pi^*$ transition which is associated with azomethine chromophore [Bella *et. al.*, 1997] was assigned to the band absorption in the higher region, between 250-349 nm. In the diorganotin complexes, this band showed a bathochromic shift due to the donation of the lone pair of electrons to the metal centre; as a result of the coordination of the azomethine group to the tin centre.

For this series of compounds, the ligand bands between 190-250 nm were assigned as $\pi \longrightarrow \pi^*$ transitions, which occurred in all the free tridentate Schiff bases ligands. This $\pi \longrightarrow \pi^*$ transition involved molecular orbitals of the C=N chromophore and the phenyl ring.

In the spectra for the organotin complexes, all the $n \rightarrow \pi^*$ type transitions, which were due to the C=N chromophore and the phenyl ring were found to shift to different wavelengths.

As the complexes had poor solubility in acetonitrile, some of the absorption bands were not visibly observed in the spectra due to the poor intensity of the band. Overall, the electronic spectra of both the ligands and diorganotin complexes were of little help in assigning a definite structure to the compounds.

Table 3.3.10
Electronic spectral data for the TRIS ligands

Ligand	Intraligand transfer transition	
	π-π^*	n-π^*
2-{[1,1-*Bis*(hydroxymethyl)-2-oxidoethyl]-iminomethyl}phenol, **TA**	216, 255	315
2-{[1,1-*Bis*(hydroxymethyl)-2-oxidoethyl]-iminomethyl}-4-bromophenol, **TB**	224, 253	327
2-{[1,1-*Bis*(hydroxymethyl)-2-oxidoethyl]-iminomethyl}-4-chlorophenol, **TC**	222, 253	326
2-{[1,1-*Bis*(hydroxymethyl)-2-oxidoethyl]-iminomethyl}-4-nitrophenol, **TD**	202	349
2-{[1,1-*Bis*(hydroxymethyl)-2-oxidoethyl]-iminomethyl}-2-methoxy-4-bromophenol, **TE**	201	323

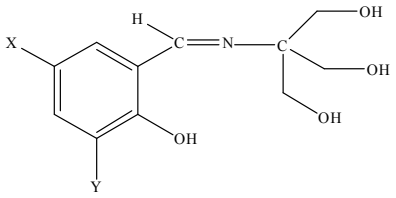

TA: X = H, Y= H ; **TB**: X = Br, Y = H;
TC: X = Cl, Y = H; **TD**: X = NO_2, Y = H;
TE: X= Br, Y = OCH_3

Table 3.3.11a
Electronic spectral data for (2-{[1,1-*bis*(hydroxymethyl)-2-oxidoethyl]-iminomethyl}phenolato)diorganotin complexes

Complex	Intraligand transfer transition	
	π-π*	n-π*
(2-{[1,1-*Bis*(hydroxymethyl)-2-oxidoethyl]-iminomethyl}phenolato)dimethyltin(IV), **TA1**	220, 240	277, 376
(2-{[1,1-*Bis*(hydroxymethyl)-2-oxidoethyl]-iminomethyl}phenolato)dibutyltin(IV), **TA2**	221, 240	278, 380
(2-{[1,1-*Bis*(hydroxymethyl)-2-oxidoethyl]-iminomethyl}phenolato)diphenyltin(IV), **TA3**	210	278, 375
(2-{[1,1-*Bis*(hydroxymethyl)-2-oxidoethyl]-iminomethyl}phenolato)dicyclohexyltin(IV), **TA4**	217, 240	278, 384
(2-{[1,1-*Bis*(hydroxymethyl)-2-oxidoethyl]-iminomethyl}phenolato)di(*o*-chlorobenzyl)tin(IV), **TA6**	242	280, 381

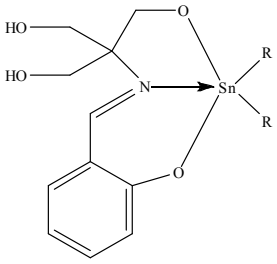

R = CH_3, C_4H_9, phenyl (Ph), cyclohexyl (Cy), benzyl (Bz), *o*-chlorobenzyl (*o*-ClBz), *p*-chlorobenzyl (*p*-ClBz)

Table 3.3.11b
Electronic spectral data for (2-{[1,1-bis(hydroxymethyl)-2-oxidoethyl]iminomethyl}-4-bromophenolato)diorganotin complexes

Complex	Intraligand transfer transition	
	π-π*	n-π*
Bis[(2-{[1,1-Bis(hydroxymethyl)-2-oxidoethyl]-iminomethyl}-4-bromophenolato)]dimethyltin(IV), **TB1**	226, 242	276, 388
(2-{[1,1-*Bis*(hydroxymethyl)-2-oxidoethyl]-iminomethyl}-4-bromophenolato)dibutyltin(IV), **TB2**	226, 242	278, 390
(2-{[1,1-*Bis*(hydroxymethyl)-2-oxidoethyl]-iminomethyl}-4-bromophenolato)diphenyltin(IV), **TB3**	218, 242	278, 387
(2-{[1,1-*Bis*(hydroxymethyl)-2-oxidoethyl]-iminomethyl}-4-bromophenolato)-dicyclohexyltin(IV), **TB4**	226	279, 397
(2-{[1,1-*Bis*(hydroxymethyl)-2-oxidoethyl]-iminomethyl}-4-bromophenolato)dibenzyltin(IV), **TB5**	*na.*	383

Note: na. = not observed

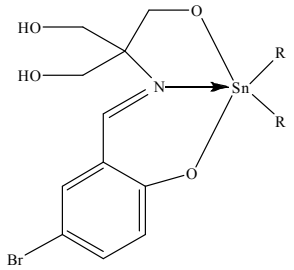

R = CH_3, C_4H_9, phenyl (Ph), cyclohexyl (Cy), benzyl (Bz), *o*-chlorobenzyl (*o*-ClBz), *p*-chlorobenzyl (*p*-ClBz)

Table 3.3.11c
Electronic spectral data for (2-{[1,1-*bis*(hydroxymethyl)-2-oxidoethyl]-iminomethyl}-4-chlorophenolato)diorganotin complexes

Complex	Intraligand transfer transition	
	π-π*	n-π*
(2-{[1,1-*Bis*(hydroxymethyl)-2-oxidoethyl]-iminomethyl}-4-chlorophenolato)dimethyltin(IV), **TC1**	229	276, 388
(2-{[1,1-*Bis*(hydroxymethyl)-2-oxidoethyl]-iminomethyl}-4-chlorophenolato)dibutyltin(IV), **TC2**	229	277, 392
(2-{[1,1-*Bis*(hydroxymethyl)-2-oxidoethyl]-iminomethyl}-4-chlorophenolato)diphenyltin(IV), **TC3**	219	278, 387
(2-{[1,1-*Bis*(hydroxymethyl)-2-oxidoethyl]-iminomethyl}-4-chlorophenolato)-dicyclohexyltin(IV), **TC4**	226	392
(2-{[1,1-*Bis*(hydroxymethyl)-2-oxidoethyl]-iminomethyl}-4-chlorophenolato)dibenzyltin(IV), **TC5**	*na.*	291, 374
(2-{[1,1-*Bis*(hydroxymethyl)-2-oxidoethyl]-iminomethyl}-4-chlorophenolato)-di(*o*-chlorobenzyl)tin(IV), **TC6**	197, 242	381

Note: na. = not observed

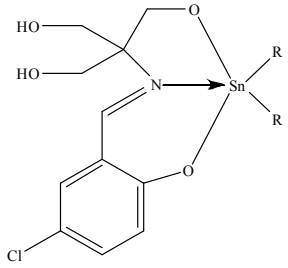

R = CH_3, C_4H_9, phenyl (Ph), cyclohexyl (Cy), benzyl (Bz), *o*-chlorobenzyl (*o*-ClBz), *p*-chlorobenzyl (*p*-ClBz)

Table 3.3.11d
Electronic spectral data for (2-{[1,1-*bis*(hydroxymethyl)-2-oxidoethyl]-iminomethyl}-4-nitrophenolato)diorganotin complexes

Complex	Intraligand transfer transition	
	π-π*	n-π*
(2-{[1,1-*Bis*(hydroxymethyl)-2-oxidoethyl]-iminomethyl}-4-nitrophenolato)dimethyltin(IV), **TD1**	na.	258, 352
(2-{[1,1-*Bis*(hydroxymethyl)-2-oxidoethyl]-iminomethyl}-4-nitrophenolato)dibutyltin(IV), **TD2**	*na.*	259, 353
(2-{[1,1-*Bis*(hydroxymethyl)-2-oxidoethyl]-iminomethyl}-4-nitrophenolato)diphenyltin(IV), **TD3**	195	258, 345
(2-{[1,1-*Bis*(hydroxymethyl)-2-oxidoethyl]-iminomethyl}-4-nitrophenolato)-dicyclohexyltin(IV), **TD4**	200	259, 353
(2-{[1,1-*Bis*(hydroxymethyl)-2-oxidoethyl]-iminomethyl}-4-nitrophenolato)dibenzyltin(IV), **TD5**	202, 237	255, 353
(2-{[1,1-*Bis*(hydroxymethyl)-2-oxidoethyl]-iminomethyl}-4-nitrophenolato)-di(*o*-chlorobenzyl)tin(IV), **TD6**	200	252, 351
(2-{[1,1-*Bis*(hydroxymethyl)-2-oxidoethyl]-iminomethyl}-4-nitrophenolato)-di(*p*-chlorobenzyl)tin(IV), **TD7**	212	*na.*

Note: na. = not observed

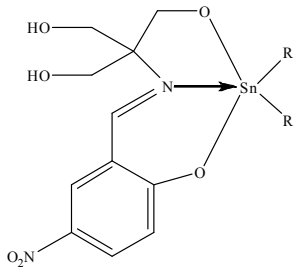

R = CH_3, C_4H_9, phenyl (Ph), cyclohexyl (Cy), benzyl (Bz), *o*-chlorobenzyl (*o*-ClBz), *p* -chlorobenzyl (*p* -ClBz)

Table 3.3.11e
Electronic spectral data for (2-{[1,1-*bis*(hydroxymethyl)-2-oxidoethyl]-iminomethyl}-2-methoxy-4-bromophenolato)diorganotin complexes

Complex	Intraligand transfer transition	
	π-π*	n-π*
(2-{[1,1-*Bis*(hydroxymethyl)-2-oxidoethyl]-iminomethyl}-2-methoxy-4-bromophenolato)-dimethyltin(IV), **TE2**	197	224
(2-{[1,1-*Bis*(hydroxymethyl)-2-oxidoethyl]-iminomethyl}-2-methoxy-4-bromophenolato)-dibutyltin(IV), **TE2**	202	244
(2-{[1,1-*Bis*(hydroxymethyl)-2-oxidoethyl]-iminomethyl}-2-methoxy-4-bromophenolato)-diphenyltin(IV), **TE3**	196	221, 349
(2-{[1,1-*Bis*(hydroxymethyl)-2-oxidoethyl]-iminomethyl}-2-methoxy-4-bromophenolato)-dicyclohexyltin(IV), **TE4**	202	230, 337
(2-{[1,1-*Bis*(hydroxymethyl)-2-oxidoethyl]-iminomethyl}-2-methoxy-4-bromophenolato)-di(*o*-chlorobenzyl)tin(IV), **TE6**	197, 212	331
(2-{[1,1-*Bis*(hydroxymethyl)-2-oxidoethyl]-iminomethyl}-2-methoxy-4-bromophenolato)-di(*p*-chlorobenzyl)tin(IV), **TE7**	197, 216	329

Note: na. = not available

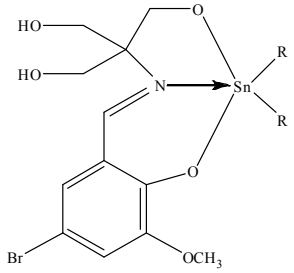

R = CH_3, C_4H_9, phenyl (Ph), cyclohexyl (Cy), benzyl (Bz), *o*-chlorobenzyl (*o*-ClBz), *p*-chlorobenzyl (*p*-ClBz)

3.3.5 X-ray Structures

Bis[(2-{[1,1-_bis_(hydroxymethyl)-2-oxidoethyl]iminomethyl}-4-bromophenolato)]dimethyltin(IV), TB1, (2-{[1,1-_bis_(hydroxymethyl)-2-oxidoethyl]iminomethyl}-4-bromophenolato)diorganotins(IV), R = Bu, Ph (TB2 and TB3)

Crystallographic data and selected bond lengths and angles for **TB1**, **TB2** and **TB3** are tabulated in tables 3.3.12 and 3.3.13 whereas the molecular structure of the complexes are shown in figures 3.3.1a, 3.3.1b and 3.3.1c respectively.

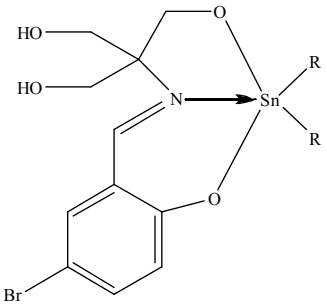

R = Me (**TB1**), Bu (**TB2**), Ph (**TB3**)

The molecular structure showed that **TB1** was a dimer (unlike the proposed structure as shown). The formation of dimeric chain in **TB1** involved one of the hydroxymethyl oxygen from each of the two adjacent molecules to form a central distannoxane Sn_2O_2 ring. The environment at both tin sites adopted distorted octahedral geometry with the imino nitrogen, the phenoxyl oxygen and two methoxyl oxygens (one of which was from the adjacent molecule) forming the equatorial plane. The sum of angles subtended at Sn(1) was 360.02^o and Sn(2) was 359.95^o respectively. These observations indicated that the square planes around both the tin atoms were flat.

The axial position was occupied by the two methyl groups and the apical angle, C(12)-Sn(1)-C(13) was 147.85(19)^{o} and C(25)-Sn(2)-C(26) was 150.8(2)^{o} respectively. The Sn(1)-O(1) and Sn(1)-O(2) bond distances were 2.262(3) Å and 2.076(3) Å, while Sn(2)-O(5) and Sn(2)-O(6) were 2.281(3) Å and 2.090(3) Å. The Sn(1)-O(2) and Sn(2)-O(6) bond distances, which were the coordination between methylene oxygen to tin, were slightly shorter than bond distances of phenoxyl oxygen to tin, Sn(1)-O(1) and Sn(2)-O(5).

Unlike **TB1**, the molecular structure of (2-{[1,1-*bis*(hydroxymethyl)-2-oxidoethyl]iminomethyl}-4-bromophenolato)dibutyltin(IV), **TB2** and (2-{[1,1-*bis*(hydroxymethyl)-2-oxidoethyl]iminomethyl}-4-bromophenolato)diphenyltin(IV), **TB3** were each monomeric. This is probably due to the steric effect introduced by the presence of the two bulky butyl and phenyl groups.

In both **TB2** and **TB3**, the ligand was tridentate in which one phenoxo, one alkoxo, an imine nitrogen atom and the two butyl chains and phenyl rings completed the coordination at tin to form a five-coordinated molecule. The equatorial plane was occupied by the imine nitrogen and the alkyl/aryl moieties of the diorganotins and the sum of angles subtended at tin for **TB2** was 359.94^{o} and 355.26^{o} for **TB3**; showing a planar trigonal plane. The apical angle, O(1)-Sn(1)-O(2), for **TB2** was 155.60(6)^{o} and **TB3** was 159.33(8)^{o} indicating that the apical angle was rather distorted from the ideal linear angle of 180^{o}. The Sn-O(1) and Sn-O(2) bond distances were 2.1203(15) Å and 2.1049(14) Å for **TB2**, 2.083(2) Å and 2.073(2) Å for **TB3** while the Sn-N bond distance was 2.2108(17) Å and 2.191(2) Å respectively. These bond distances were within the range of bond distances reported in the literature for Sn-O and Sn-N coordination.

Figure 3.3.1a
Molecular plot of *bis*[(2-{[1,1-*bis*(hydroxymethyl)-2-oxidoethyl]iminomethyl}-4-bromophenolato)]dimethyltin(IV), **TB1**

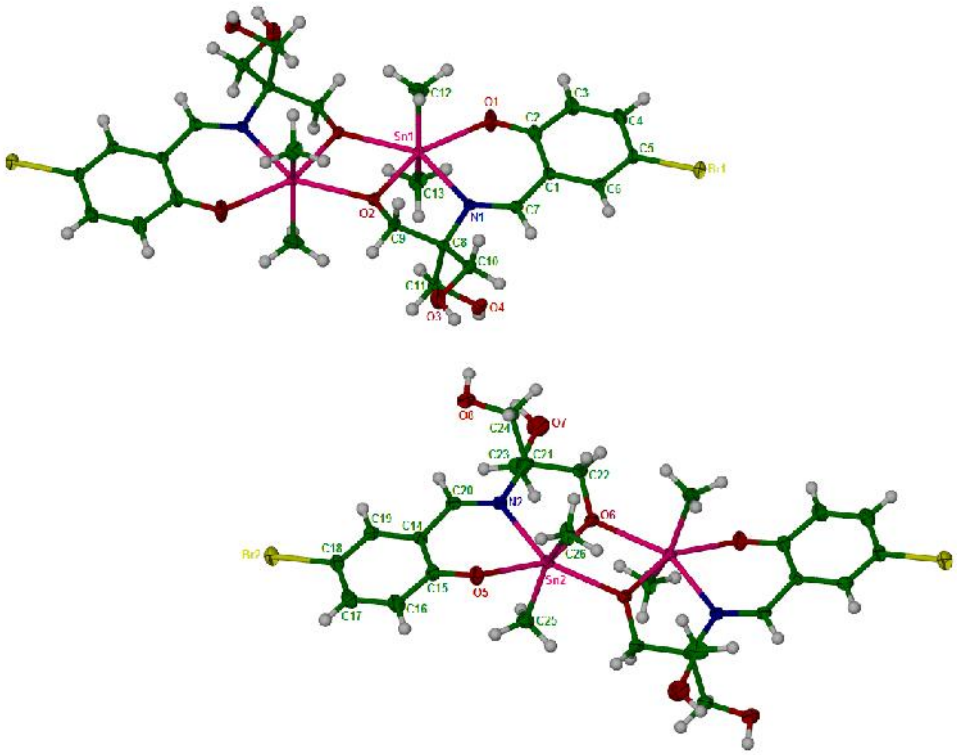

Figure 3.3.2a
Packing diagram of *bis*[(2-{[1,1-*bis*(hydroxymethyl)-2-oxidoethyl]iminomethyl}-4-bromophenolato)]dimethyltin(IV), **TB1**, showing hydrogen bonding between O(1) with O(3)-H, O(4) with O(8)-H and O(5) with O(4)-H

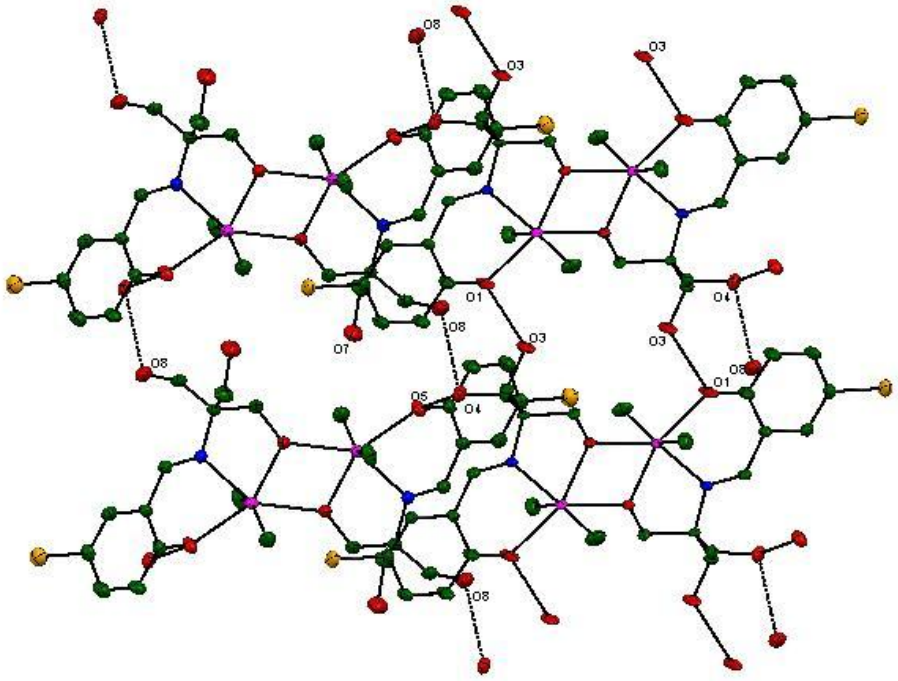

Figure 3.3.1b
Molecular plot of (2-{[1,1-*bis*(hydroxymethyl)-2-oxidoethyl]iminomethyl}-4-bromophenolato)dibutyltin(IV), **TB2**

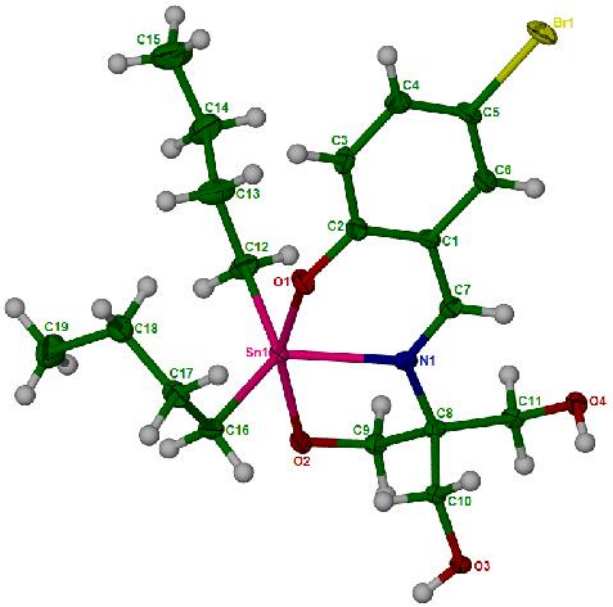

Figure 3.3.2b
Packing diagram of (2-{[1,1-*bis*(hydroxymethyl)-2-oxidoethyl]iminomethyl}-4-bromophenolato)dibutyltin(IV), **TB2**, showing hydrogen bonding between O(2) with O(3)-H and O(3) with O(4)-H

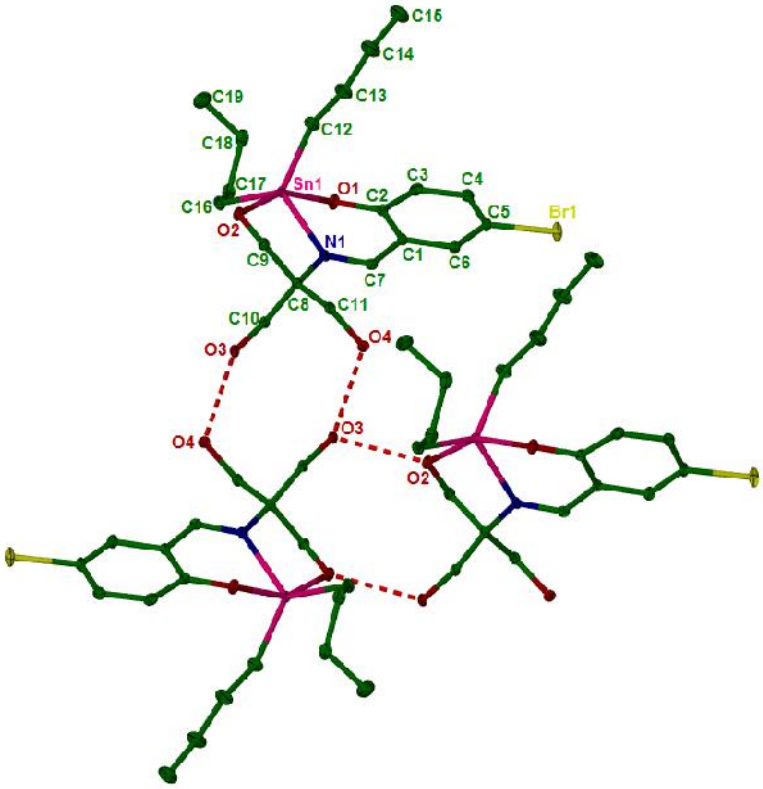

Figure 3.3.1c
Molecular plot of (2-{[1,1-*bis*(hydroxymethyl)-2-oxidoethyl]iminomethyl}-4-bromophenolato)diphenyltin(IV), **TB3**

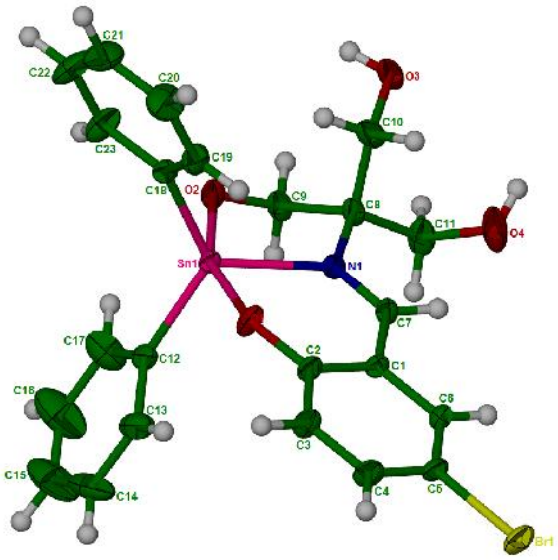

Figure 3.3.2c
Packing diagram of (2-{[1,1-*bis*(hydroxymethyl)-2-oxidoethyl]iminomethyl}-4-bromophenolato)diphenyltin(IV), **TB3**, showing hydrogen bonding between O(2) with O(3)-H and O(3) with O(4)-H

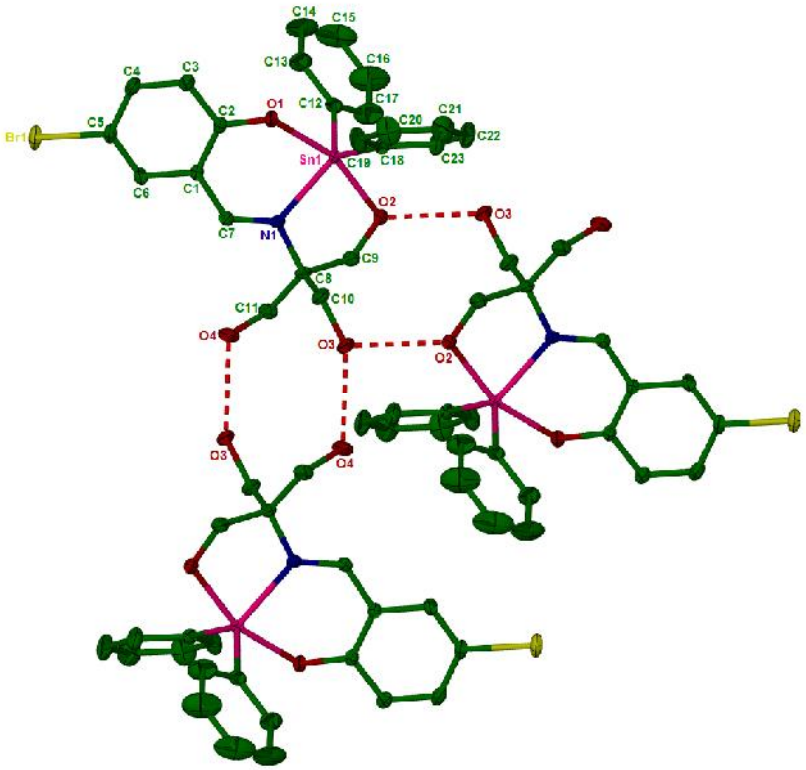

Table 3.3.12
Crystallographic parameters for complexes **TB1**, **TB2** and **TB3**

	TB1	**TB2**	**TB3**
Empirical formula	$C_{26}H_{36}Br_2N_2O_8Sn_2$	$C_{19}H_{30}BrNO_4Sn$	$C_{23}H_{22}BrNO_4Sn$
Formula weight	901.77	535.04	575.02
Crystal system	Monoclinic	Monoclinic	Triclinic
Space group	$P2_1/n$	$C2/c$	$P\bar{1}$
a (Å)	18.9301(4)	18.8326(9)	8.7156(2)
b (Å)	8.8951(2)	13.3811(7)	10.0110(3)
c (Å)	19.8873(4)	16.5768(8)	14.8031(4)
α (^{o})	90	90	104.680(1)
β (^{o})	114.075(1)	91.385(3)	94.759(1)
γ (^{o})	90	90	113.230(1)
Volume (Å^3)	3057.43(11)	5214.9(3)	1123.57(5)
Z	4	8	2
Calculated density, D_{calc} (Mgm^{-3})	1.959	1.702	1.700
Absorption coefficient, μ (mm^{-1})	4.297	3.160	2.944
F(000)	1760	2144	568
Crystal size (mm)	0.40 x 0.33 x 0.27	0.40 x 0.10 x 0.08	0.43 x 0.40 x 0.36
Limiting indices	$-24 \le h \le 24$, $-11 \le k \le 9$, $-25 \le l \le 25$	$-24 \le h \le 24$, $-17 \le k \le 17$, $-21 \le l \le 21$	$-11 \le h \le 9$, $-12 \le k \le 12$, $-19 \le l \le 19$

Reflections collected / unique	21362 / 7016 [$R_{(int)}$ = 0.0279]	19535 / 4785 [$R_{(int)}$ = 0.0324]	8208 / 5038 [$R_{(int)}$ = 0.0181]
Max. and min. transmission	0.3900 and 0.2783	0.7861 and 0.3646	0.4171 and 0.3642
Data / restraints / parameters	7016 / 0 / 365	4785 / 2 / 239	5038 / 0 / 274
Goodness-of-fit on F^2	1.158	1.023	1.163
Final R indices [$I>2\sigma(I)$]	R_1 = 0.0293, wR_2 = 0.0846	R_1 = 0.0218, wR_2 = 0.0494	R_1 = 0.0239, wR_2 = 0.0706
R indices (all data)	R_1 = 0.0394, wR_2 = 0.1052	R_1 = 0.0274, wR_2 = 0.051	R_1 = 0.0286, wR_2 = 0.0900
Largest diff. peak and hole ($eÅ^{-3}$)	1.595 and -1.087	0.647 and -0.375	0.749 and -0.793

Table 3.3.13
Selected bond lengths (Å) and angles (°) with estimated standard deviation for complexes **TB1**, **TB2** and **TB3**

	TB1	**TB2**	**TB3**
Bond lengths			
Sn(1)-O(1)	2.262(3), 2.281(3)	2.120(3)	2.083(2)
Sn(1)-O(2)	2.075(2), 2.090(3)	2.1049(14)	2.073(2)
Sn(1)-O(2)#	2.329(2), 2.348(3)	-	-
Sn(1)-N(1)	2.269(3), 2.269(3)	2.2108(17)	2.191(2)
Sn(1)-C_i	2.113(4), 2.117(4)	2.129(2)	2.123(3)
Sn(1)-C_i'	2.113(4), 2.109(4)	2.139(2)	2.125(3)
C(2)-O(1)	1.291(5), 1.320(5)	1.317(2)	1.319(3)
C(9)-O(2)	1.403(4), 1.405(5)	1.405(2)	1.403(4)
C(10)-O(3)	1.400(4), 1.408(5)	1.422(2)	1.411(3)
C(11)-O(4)	1.419(4), 1.409(5)	1.418(2)	1.406(4)
C(7)-N(1)	1.296(4), 1.285(5)	1.289(3)	1.292(4)
C(8)-N(1)	1.479(4), 1.475(5)	1.487(3)	1.485(3)
Bond angles			
O(1)-Sn(1)-O(2)	155.32(10), 152.04(10)	155.60(6)	159.33(8)
C_i-Sn(1)- C_i'	147.94(18), 150.87(19)	129.92(9)	120.80(2)
N(1)-Sn(1)- C_i	105.06(15), 99.65(15)	107.69(8)	112.97(10)
N(1)-Sn(1)- C_i'	100.46(14), 103.03(16)	122.33(7)	121.49(10)

Note:
C_i and C_i'refer to the *ipso*-carbon of the diorganotin moieties attached to the central tin

(2-{[1,1-*Bis*(hydroxymethyl)-2-oxidoethyl]iminomethyl}-4-chlorophenolato)-diorganotins(IV), R = Me, Ph and Cy (TC1, TC3 and TC4)

The molecular structures of the complexes are shown in figures 3.3.3a, 3.3.3b and 3.3.3c respectively while the crystallographic data and selected bond lengths and angles are tabulated in tables 3.3.14 and 3.3.15.

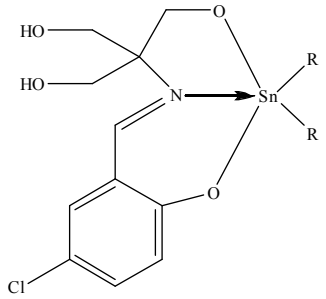

R = Me (**TC1**), Ph (**TC3**), Cy (**TC4**)

From their molecular plots, the tin atoms were found to adopt distorted trigonal-bipyramidal geometry, whereby the trigonal plane consisted of the imine nitrogen and two alkyl/aryl groups from the diorganotin moieties. The sum of angles subtended at tin for **TC1** was 359.86^{o}, **TC3** was 359.85^{o} and **TC4** were 359.9^{o} and 360^{o} respectively. The axial position which was occupied by the phenoxyl and methoxyl oxygens had a O(1)-Sn(1)-O(2) angle of 158.37(6)^{o} for **TC1**, 159.03(7)^{o} for **TC3** and 156.46(17)^{o} and 158.29(16)^{o} for **TC4**. These values showed that the apical angle of the complexes was largely dependent on the size of the alkyl/aryl groups of the diorganotin moieties.

As similar to **TB3**, (2-{[1,1-*bis*(hydroxymethyl)-2-oxidoethyl]iminomethyl}-4-chlorophenolato)diphenyltin(IV), **TC3** also crystallizes in triclinic, $P\bar{1}$ space group. In the case of (2-{[1,1-*bis*(hydroxymethyl)-2-oxidoethyl]iminomethyl}-4-

chlorophenolato)dicyclohexyltin(IV), **TC4**, there were two unique molecules in its asymmetric unit.

The Sn-O(1) and Sn-O(2) bond distances of these complexes were within the values of those reported for five-coordinated diorganotin complexes [**TC1**: 2.1251(16) Å and 2.0752(15) Å, **TC3**: 2.0920(17) Å and 2.0821(2) Å, **TC4**: 2.076(5) Å, 2.093(4) Å, 2.131(4) Å and 2.107(4) Å respectively] while the Sn(1)-N(1) bond distance was between 2.19-2.20 Å.

All three complexes were monomeric and in the crystal structure, the molecules in each of the complexes were linked together by strong intermolecular hydrogen bonding.

Figure 3.3.3a
Molecular plot of (2-{[1,1-*bis*(hydroxymethyl)-2-oxidoethyl]iminomethyl}-4-chlorophenolato)dimethyltin(IV), **TC1**

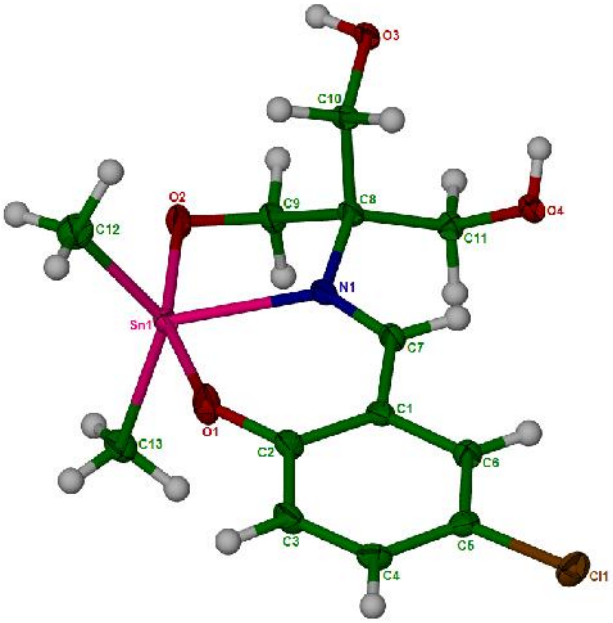

Figure 3.3.4a
Packing diagram of (2-{[1,1-*bis*(hydroxymethyl)-2-oxidoethyl]iminomethyl}-4-chlorophenolato)dimethyltin(IV), **TC1**, showing hydrogen bonding between O(2) with O(3)-H and O(3) with O(4)-H

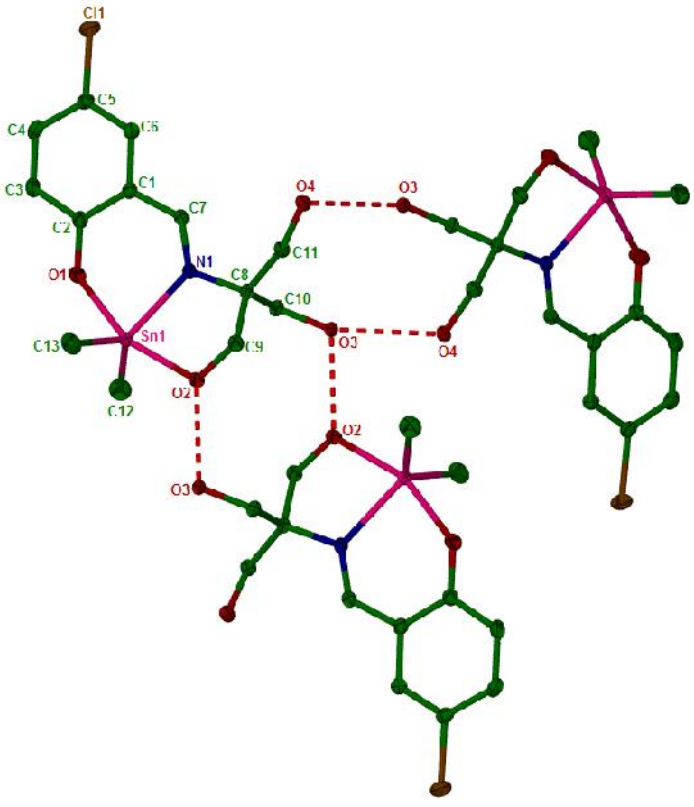

Figure 3.3.3b
Molecular plot of (2-{[1,1-*bis*(hydroxymethyl)-2-oxidoethyl]iminomethyl}-4-chlorophenolato)diphenyltin(IV), **TC3**

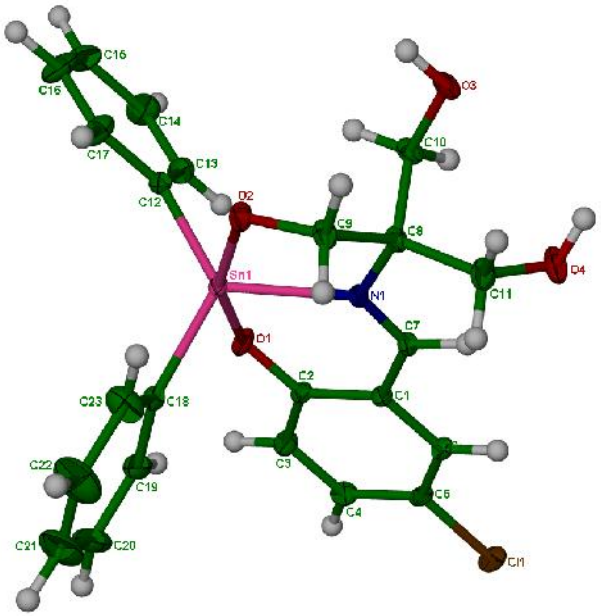

Figure 3.3.4b
Packing diagram of (2-{[1,1-*bis*(hydroxymethyl)-2-oxidoethyl]iminomethyl}-4-chlorophenolato)diphenyltin(IV), **TC3**, showing hydrogen bonding between O(2) with O(3)-H and O(3) with O(4)-H

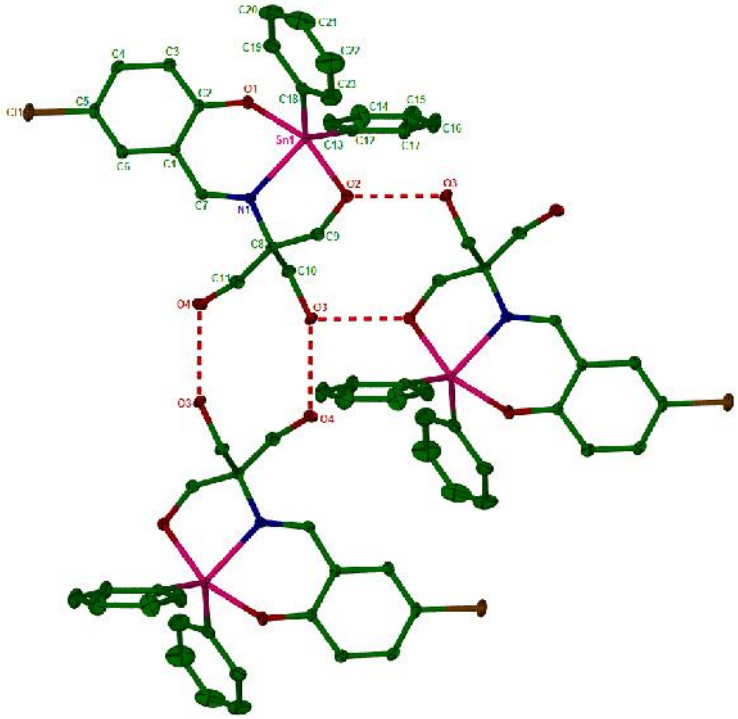

Figure 3.3.3c
Molecular plot of (2-{[1,1-*bis*(hydroxymethyl)-2-oxidoethyl]iminomethyl}-4-chlorophenolato)dicyclohexyltin(IV), **TC4**

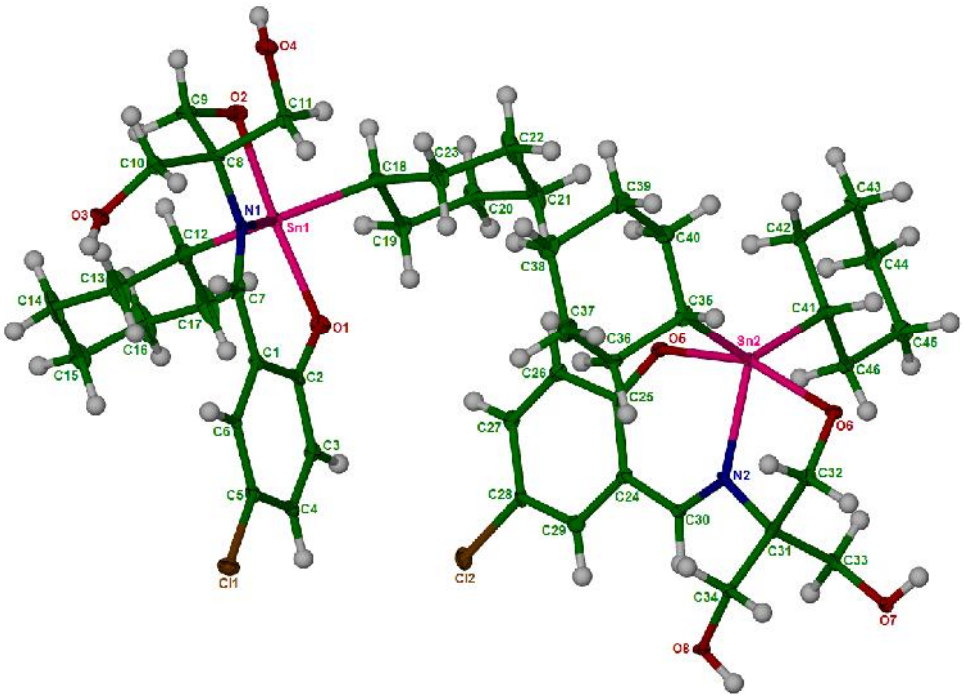

Figure 3.3.4c
Packing diagram of (2-{[1,1-*bis*(hydroxymethyl)-2-oxidoethyl]iminomethyl}-4-chlorophenolato)dicyclohexyltin(IV), **TC4**, showing hydrogen bonding between O(2) with O(8)-H, O(6) with O(7)-H and O(7) with O(4)-H

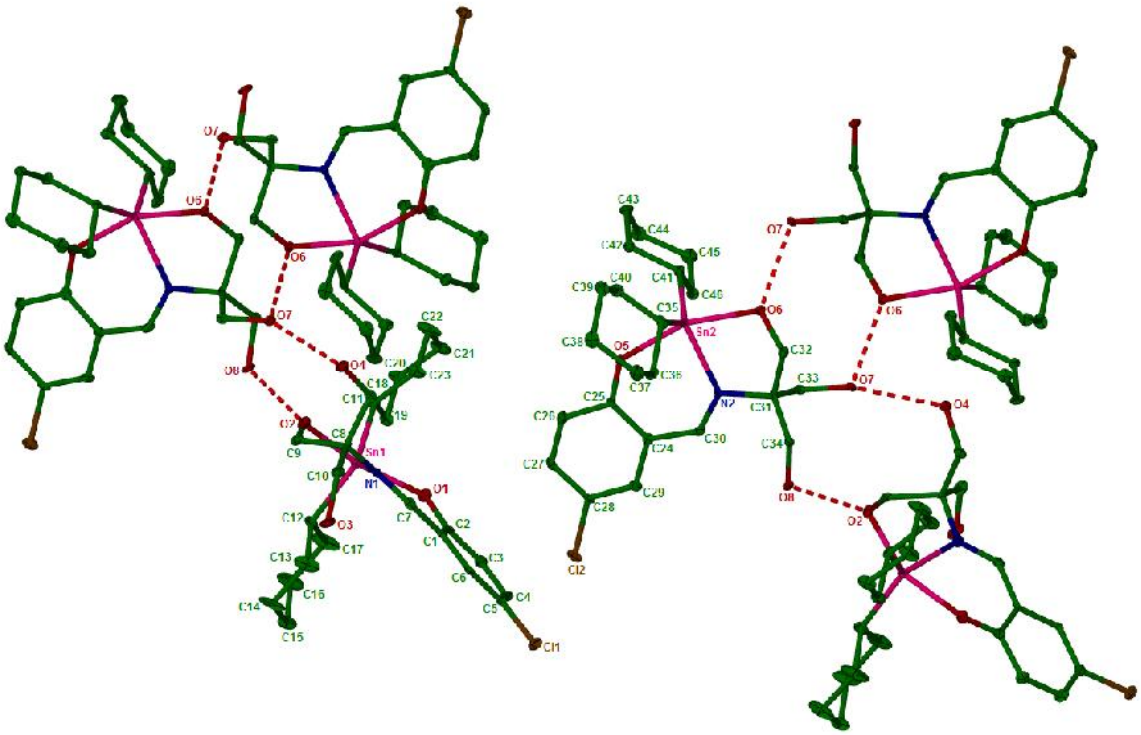

Table 3.3.14
Crystallographic parameters for complexes **TC1**, **TC3** and **TC4**

	TC1	**TC3**	**TC4**
Empirical formula	$C_{13}H_{18}ClNO_4Sn$	$C_{23}H_{22}ClNO_4Sn$	$C_{23}H_{34}ClNO_4Sn$
Formula weight	406.42	530.56	542.65
Crystal system	Monoclinic	Triclinic	Monoclinic
Space group	C2/c	$P\bar{1}$	$P2_1/n$
a (Å)	14.8956(6)	8.6518(3)	17.0881(4)
b (Å)	13.8128(5)	9.9622(4)	12.6893(4)
c (Å)	16.7610(6)	15.0439(6)	22.1755(6)
α (^{o})	90	100.9511(16)	90
β (^{o})	114.299(2)	102.8430(15)	97.778(2)
γ (^{o})	90	113.1112(13)	90
Volume (Å^3)	3143.1(2)	1105.79(7)	4764.2(2)
Z	8	2	8
Calculated density, D_{calc} (Mgm^{-3})	1.718	1.593	1.513
Absorption coefficient, μ (mm^{-1})	1.807	1.305	1.213
F(000)	1616	532	2224
Crystal size (mm)	0.45 x 0.34 x 0.06	0.45 x 0.34 x 0.06	0.15 x 0.15 x 0.05
Limiting indices	$-19 \le h \le 18$, $-17 \le k \le 17$, $-21 \le l \le 21$	$-11 \le h \le 9$, $-12 \le k \le 12$, $-16 \le l \le 19$	$-20 \le h \le 20$, $-15 \le k \le 15$, $-26 \le l \le 26$

Reflections collected / unique	16984 / 3594 [$R_{(int)}$ = 0.0268]	9422 / 4973 [$R_{(int)}$ = 0.0158]	37000 / 8392 [$R_{(int)}$ = 0.1372]
Max. and min. transmission	0.8993 and 0.4969	0.9258 and 0.5912	0.9418 and 0.8390
Data / restraints / parameters	3594 / 2 / 191	4973 / 0 / 273	8392 / 0 / 545
Goodness-of-fit on F^2	1.242	1.340	1.001
Final R indices [I>2σ(I)]	R_1 = 0.0180, wR_2 = 0.0544	R_1 = 0.0197, wR_2 = 0.0596	R_1 = 0.0529, wR_2 = 0.0860
R indices (all data)	R_1 = 0.0210, wR_2 = 0.0677	R_1 = 0.0257, wR_2 = 0.0968	R_1 = 0.1103, wR_2 = 0.1045
Largest diff. peak and hole ($eÅ^{-3}$)	0.745 and -0.460	0.662 and -1.165	0.676 and -0.675

Table 3.3.15
Selected bond lengths (Å) and angles (°) with estimated standard deviation for complexes **TC1**, **TC3** and **TC4**

	TC1	**TC3**	**TC4**
Bond lengths			
Sn(1)-O(1)	2.1251(16)	2.0920(17)	2.093(4), 2.131(4)
Sn(1)-O(2)	2.0752(15)	2.0821(17)	2.076(5), 2.107(4)
Sn(1)-N(1)	2.2090(17)	2.1967(19)	2.215(6), 2.196(5)
Sn(1)-C_i	2.117(2)	2.129(2)	2.143(6), 2.143(6)
Sn(1)-C_i'	2.117(2)	2.130(2)	2.147(7), 2.133(7)
C(2)-O(1)	1.312(3)	1.314(3)	1.315(7), 1.315(7)
C(9)-O(2)	1.413(2)	1.414(3)	1.401(8), 1.401(7)
C(10)-O(3)	1.413(3)	1.416(3)	1.486(8), 1.417(7)
C(11)-O(4)	1.421(3)	1.408(3)	1.415(8), 1.416(7)
C(7)-N(1)	1.300(3)	1.293(3)	1.295(8), 1.301(7)
C(8)-N(1)	1.492(3)	1.490(3)	1.426(7), 1.512(7)
Bond angles			
O(1)-Sn(1)-O(2)	158.37(6)	159.03(7)	156.46(17), 158.29(16)
C_i-Sn(1)- C_i'	125.83(9)	126.60(9)	122.2(3), 132.9(3)
N(1)-Sn(1)- C_i	119.51(8)	121.86(8)	110.4(2), 118.6(2)
N(1)-Sn(1)- C_i'	114.52(8)	111.39(8)	127.3(2), 108.5(2)

Note:
C_i and C_i'refer to the *ipso*-carbon of the diorganotin moieties attached to the central tin atom

Summary

Although both **TB1** and **TC1** were dimethyltin derivatives, the complexes showed different molecular arrangement; **TB1** was a dimer while **TC1** was monomeric. The difference between the two complexes could also be observed from the O(1)-Sn(1)-O(2) angle, whereby the angle was smaller in **TB1** [O(1)-Sn(1)-O(2) is 155.32(10)^{o}] compared to **TC1** [O(1)-Sn(1)-O(2) is 158.37(6)^{o}]. The Sn-O bond distances for **TB3** and **TC3,** which were diphenyltin derivatives, were shorter than their dimethyltin and dibutyltin derivatives.

Strong intermolecular O-H---O hydrogen bonding interactions were observed in all the diorganotin complexes. There were two different hydrogen bondings observed in complex **TB1**; that was between the phenoxyl oxygen and one of the free methoxyl oxygen and between the methoxyl oxygen with the free methoxyl oxygen from an adjacent molecule. For complexes **TB2**, **TB3**, **TC1**, **TC3** and **TC4**, the hydrogen bondings involved two different pairs of free methoxyl oxygen with the free methoxyl oxygen from an adjacent molecule. The hydrogen bonding interactions are indicated in the molecular structures in the packing diagrams [Complex **TB1**: O-H..O 3.117(5), 2.697(4), 2.705(4) and 2.703(4) Å; Complex **TB2**: O-H..O 2.608(2) and 2.733(2) Å; Complex **TB3**: O-H..O 2.623(3) and 2.666(3) Å; Complex **TC1**: O-H..O 2.620(2) and 2.707(2) Å; Complex **TC3**: O-H..O 2.639(2) and 2.695(3) Å]. The hydrogen bonding which linked the molecules resulted in the formation of infinite polymeric structures.

3.4. Cytotoxic Activity

The *in vitro* cytotoxic activity of the Schiff base ligands and their diorganotin complexes had been evaluated against three human carcinoma cell lines, namely HT-29 (human colon carcinoma cell line), SKOV-3 (human ovarian cancer cell line) and MCF-7 (hormone-dependent breast carcinoma cell line). For the anticancer screening, the Schiff base ligands and diorganotin complexes were dissolved in DMSO. The concentration of DMSO used did not reveal any cytotoxic activity.

Cisplatin used as a positive control in the present study was found to exhibit remarkable growth inhibitory activities with mean IC_{50} values ranging from 1.4-5.7 μg mL^{-1} on the studied cancer cell lines. The diorganotin complexes in general displayed better cytotoxicity against the tested human carcinoma cell lines as compared to the Schiff base ligands.

From the tabulated data, it could be observed that the Schiff base ligands were less cytotoxic in all the tested cell lines. In fact, the ligands hardly killed any of the cancer cells. The dibenzyltin and di(*p*-chlorobenzyl)tin derivatives also displayed poor cytotoxicity in all the tested cancer-lines.

In **TA** series, the dicyclohexyltin derivative, **TA4** was not tested for its biological activity as the yield obtained from the preparation of the complex was low. As observed from table 3.4.1a, only the dibutyltin derivative, **TA2** and diphenyltin derivative, **TA3** showed prominent cytotoxic activity. The dimethyltin derivative, **TA1** was only active against the MCF-7 cell line.

For **TB** series, the dimethyltin, dibenzyltin and di(*p*-chlorobenzyl)tin derivatives were found to be inactive in all the tested cell lines. The dicyclohexyltin derivative, **TB4**, was the most active compound, followed by the dibutyltin derivative, **TB2** and diphenyltin derivative, **TB3**, as observed from the results against HT-29 and MCF-7 cell lines. The three compounds displayed similar anticancer activities in SKOV-3 cell lines.

Similarly, in **TC** series, dimethyltin, dibenzyltin and di(*p*-chlorobenzyl)tin derivatives were also not active against all the tested cell lines with IC_{50} values of more than 100 μg ml^{-1}. Only the dibutyltin, diphenyltin and dicyclohexyltin derivatives were active against the three tested cancer cell-lines. From table 3.4.1c, it is noted that the dibutyltin derivative, **TC2**, was the most active against the MCF-7 cell line while the dicyclohexyltin derivative, **TC4**, was more active against HT-29 cell line. The diphenyltin derivative, **TC3**, was the least active compound against the HT-29 cell line.

In conclusion, the cytotoxic activities of the tested TRIS Schiff ligands and their diorganotin complexes were not as good as compared to the *cisplatin*. This was probably due to the insolubility of the ligands and the diorganotin complexes in most solvents including water. Although the TRIS Schiff base ligands and complexes contained several free hydroxyl groups in their molecular structures, the presence of strong intramolecular and intermolecular hydrogen bonding could be affecting the solubility of the ligands and complexes.

Table 3.4.1a
Cytotoxic activity of of 2-{[1,1-*bis*(hydroxymethyl)-2-oxidoethyl]iminomethyl}-phenol, **TA** and (2-{[1,1-*bis*(hydroxymethyl)-2-oxidoethyl]iminomethyl}-phenolato)diorganotin(IV) complexes

Compound	Cell lines (IC_{50} μg ml^{-1})[a]		
	HT-29	**MCF-7**	**SKOV-3**
cisplatin	5± 0	2.4 ± 0.6	1.4 ± 0
2-{[1,1-*Bis*(hydroxymethyl)-2-oxidoethyl]iminomethyl}phenol, **TA**	> 100	> 100	> 100
(2-{[1,1-*Bis*(hydroxymethyl)-2-oxidoethyl]-iminomethyl}phenolato)dimethyltin(IV), **TA1**	> 100	5.7 ± 0.6	> 100
(2-{[1,1-*Bis*(hydroxymethyl)-2-oxidoethyl]-iminomethyl}phenolato)dibutyltin(IV), **TA2**	6.7 ± 0.1	1.6 ± 0.3	2.2 ± 0.2
(2-{[1,1-*Bis*(hydroxymethyl)-2-oxidoethyl]-iminomethyl}phenolato)diphenyltin(IV), **TA3**	65.2 ± 1.3	46.7 ± 1.2	36 ± 0.5
(2-{[1,1-*Bis*(hydroxymethyl)-2-oxidoethyl]-iminomethyl}phenolato)dibenzyltin(IV), **TA5**	> 100	> 100	> 100
(2-{[1,1-*Bis*(hydroxymethyl)-2-oxidoethyl]-iminomethyl}phenolato)di(*p*-chlorobenzyl)tin(IV), **TA7**	> 100	> 100	> 100

[a] IC_{50} values (μg ml^{-1}) = inhibition concentration at 50% *i.e.*, the concentration to reduce growth of cancer cells by 50%

Graph 3.4.1a
Bar chart showing IC_{50} value of 2-{[1,1-*bis*(hydroxymethyl)-2-oxidoethyl]-iminomethyl}phenol, **TA** and (2-{[1,1-*bis*(hydroxymethyl)-2-oxidoethyl]iminomethyl}-phenolato)diorganotin(IV) complexes

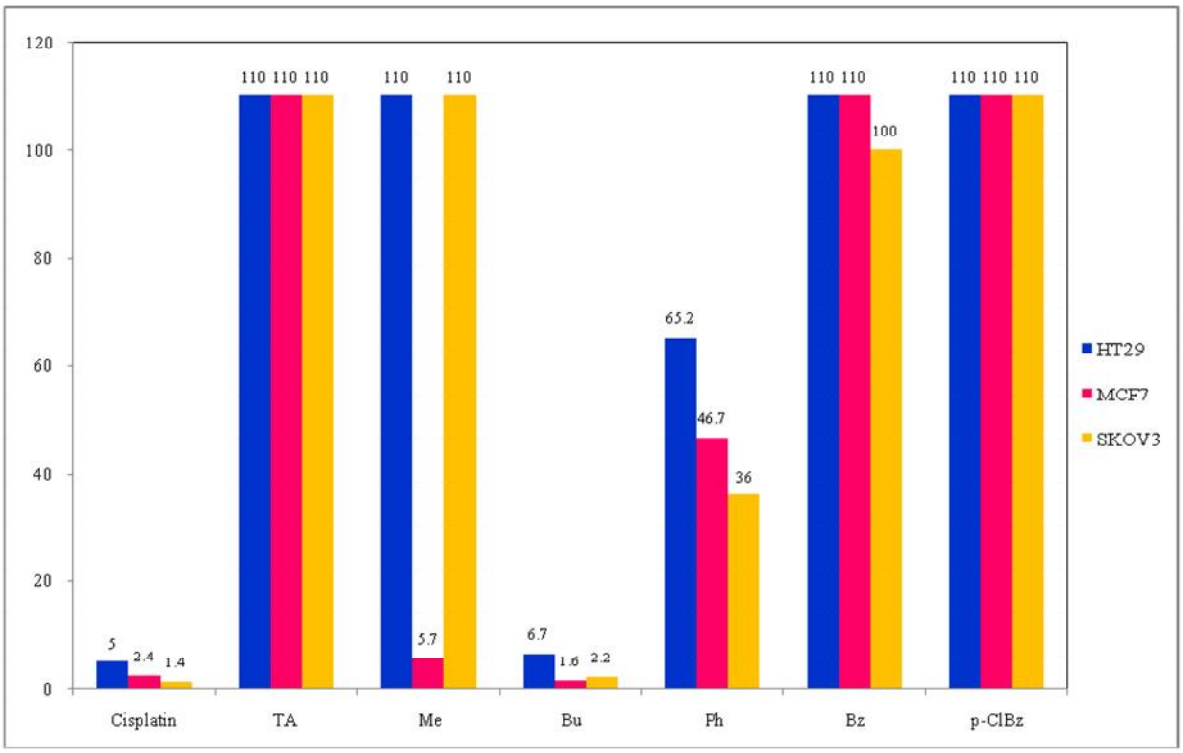

Table 3.4.1b
Cytotoxic activity of 2-{[1,1-*bis*(hydroxymethyl)-2-oxidoethyl]iminomethyl}-4-bromophenol, **TB** and (2-{[1,1-*bis*(hydroxymethyl)-2-oxidoethyl]iminomethyl}-4-bromophenolato)diorganotin(IV) complexes

Compound	Cell lines (IC_{50} μg ml^{-1})[a]		
	HT-29	**MCF-7**	**SKOV-3**
Cisplatin	5± 0	2.4 ± 0.6	1.4 ± 0
2-{[1,1-*Bis*(hydroxymethyl)-2-oxidoethyl]iminomethyl}-4-bromophenol, **TB**	> 100	> 100	83.3 ± 0.8
Bis[(2-{[1,1-*Bis*(hydroxymethyl)-2-oxidoethyl]-iminomethyl}-4-bromophenolato)]dimethyltin(IV), **TB1**	> 100	> 100	72.3 ± 0.3
(2-{[1,1-*Bis*(hydroxymethyl)-2-oxidoethyl]-iminomethyl}-4-bromophenolato)dibutyltin(IV), **TB2**	35.3 ± 0.6	6.7 ± 0.1	5.7 ± 0.1
(2-{[1,1-*Bis*(hydroxymethyl)-2-oxidoethyl]-iminomethyl}-4-bromophenolato)diphenyltin(IV), **TB3**	34.7 ± 0.6	27.7 ± 0.3	5.6 ± 0.1
(2-{[1,1-*Bis*(hydroxymethyl)-2-oxidoethyl]-iminomethyl}-4-bromophenolato)dicyclohexyltin(IV), **TB4**	7.1 ± 0.3	3.57 ± 0.15	5.7 ± 0.1
(2-{[1,1-*Bis*(hydroxymethyl)-2-oxidoethyl]-iminomethyl}-4-bromophenolato)dibenzyltin(IV), **TB5**	> 100	> 100	> 100
(2-{[1,1-*Bis*(hydroxymethyl)-2-oxidoethyl]imino-methyl}-4-bromophenolato)di(*p*-chlorobenzyl)tin(IV), **TB7**	> 100	> 100	> 100

[a] IC_{50} values (μg ml^{-1}) = inhibition concentration at 50% *i.e.*, the concentration to reduce growth of cancer cells by 50%

Graph 3.4.1b
Bar chart showing IC_{50} value of 2-{[1,1-*bis*(hydroxymethyl)-2-oxidoethyl]iminomethyl}-4-bromophenol, **TB** and (2-{[1,1-*bis*(hydroxymethyl)-2-oxidoethyl]iminomethyl}-4-bromophenolato)diorganotin(IV) complexes

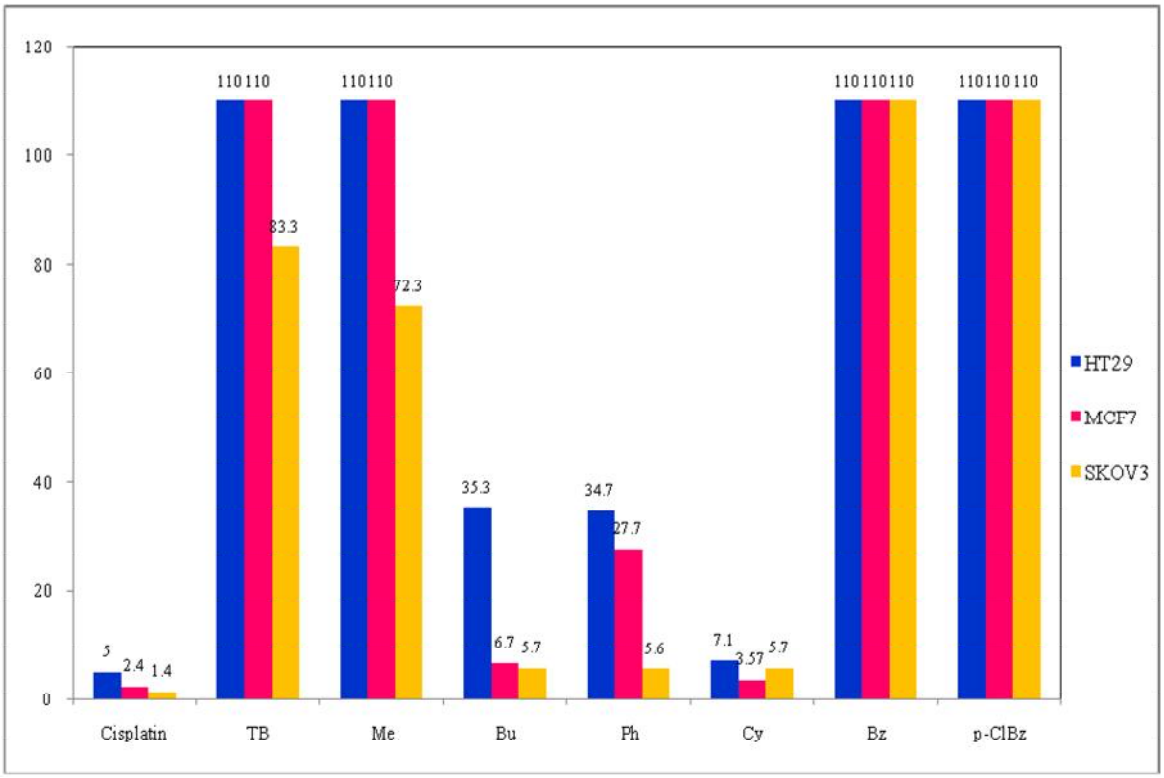

Table 3.4.1c
Cytotoxic activity of 2-{[1,1-*bis*(hydroxymethyl)-2-oxidoethyl]iminomethyl}-4-chlorophenol, **TC** and (2-{[1,1-*bis*(hydroxymethyl)-2-oxidoethyl]iminomethyl}-4-chlorophenolato)diorganotin(IV) complexes

Compound	Cell lines (IC_{50} μg ml^{-1})[a]		
	HT-29	**MCF-7**	**SKOV-3**
cisplatin	5± 0	2.4 ± 0.6	1.4 ± 0
2-{[1,1-*Bis*(hydroxymethyl)-2-oxidoethyl]iminomethyl}-4-chlorophenol, **TC**	> 100	> 100	100 ± 0
(2-{[1,1-*Bis*(hydroxymethyl)-2-oxidoethyl]-iminomethyl}-4-chlorophenolato)dimethyltin(IV), **TC1**	> 100	> 100	> 100
(2-{[1,1-*Bis*(hydroxymethyl)-2-oxidoethyl]-iminomethyl}-4-chlorophenolato)dibutyltin(IV), **TC2**	8.2 ± 0.2	2.2 ± 1.2	5.6 ± 0.1
(2-{[1,1-*Bis*(hydroxymethyl)-2-oxidoethyl]-iminomethyl}-4-chlorophenolato)diphenyltin(IV), **TC3**	41 ± 1	7.9 ± 0.1	5.7 ± 0
(2-{[1,1-*Bis*(hydroxymethyl)-2-oxidoethyl]-iminomethyl}-4-chlorophenolato)dicyclohexyltin(IV), **TC4**	4.6 ± 0.1	8.2 ± 0.2	5.4 ± 0.1
(2-{[1,1-*Bis*(hydroxymethyl)-2-oxidoethyl]-iminomethyl}-4-chlorophenolato)dibenzyltin(IV), **TC5**	> 100	> 100	> 100
(2-{[1,1-*Bis*(hydroxymethyl)-2-oxidoethyl]-iminomethyl}-4-chlorophenolato)-di(*p*-chlorobenzyl)tin(IV), **TC7**	> 100	> 100	> 100

[a] IC_{50} values (μg ml^{-1}) = inhibition concentration at 50% *i.e.*, the concentration to reduce growth of cancer cells by 50%

Graph 3.4.1c
Bar chart showing IC_{50} value of 2-{[1,1-*bis*(hydroxymethyl)-2-oxidoethyl]iminomethyl}-4-chlorophenol, **TC** and (2-{[1,1-*bis*(hydroxymethyl)-2-oxidoethyl]iminomethyl}-4-chlorophenolato)diorganotin(IV) complexes